

Article

Power Quality Detection and Categorization Algorithm Actuated by Multiple Signal Processing Techniques and Rule-Based Decision Tree

Surendra Singh ¹, Avdhesh Sharma ¹, Akhil Ranjan Garg ¹, Om Prakash Mahela ^{2,3}, Baseem Khan ^{3,4,*}, Ilyes Boulkaibet ^{5,*}, Bilel Neji ⁵, Ahmed Ali ⁶ and Julien Brito Ballester ^{7,8}

¹ Department of Electrical Engineering, MBM University, Jodhpur 342001, India

² Power System Planning Division, Rajasthan Rajya Vidyut Prasaran Nigam Ltd., Jaipur 302005, India

³ Engineering Research and Innovation Group (ERIG), Universidad Internacional Iberoamericana, Campeche 24560, Mexico

⁴ Department of Electrical Engineering, Hawassa University, Hawassa 1530, Ethiopia

⁵ College of Engineering and Technology, American University of the Middle East, Egaila 54200, Kuwait

⁶ Department of Electrical and Electronic Engineering Technology, Faculty of Engineering and the Built Environment, University of Johannesburg, Johannesburg P.O. Box 524, South Africa

⁷ Faculty of Social Sciences and Humanities, Universidad Europea del Atlántico, C/Isabel Torres 21, 39011 Santander, Spain

⁸ Faculty of Social Sciences and Humanities, Universidad Internacional Iberoamericana, Campeche 24560, Mexico

* Correspondence: baseem.khan04@gmail.com (B.K.); ilyes.boulkaibet@aum.edu.kw (I.B.)

Abstract: This paper introduces a power quality (PQ) detection and categorization algorithm actuated by multiple signal processing techniques and rule-based decision tree (RBDT). This is aimed to recognize PQ events of simple nature and higher order multiplicity with less computational time using hybridization of the signal processing techniques. A voltage waveform with a PQ event (PQE) is processed using the Stockwell transform (ST) to compute the Stockwell PQ detection index (SPDI). The voltage waveform is also processed using the Hilbert transform (HT) to compute the Hilbert PQ detection index (HPDI). A voltage waveform is also decomposed using the Discrete Wavelet transform (DWT) to compute the classification feature index (CFI) [CFI1 to CFI4]. A combined PQ detection index (CPDI) is computed by multiplication of the SPDI, the HPDI and CFI1 to CFI4. Incidence of a PQE on a voltage signal is located with the help of a location PQ disturbance index (LPDI) which is computed by differentiating the CPDI with respect to time. CFI5, CFI6 and CFI7 are computed from the SPDI, the HPDI and the CPDI, respectively. Categorization of PQ events is performed using CFI1 to CFI7 by the rule-based decision tree (RBDT) with the help of simple decision rules. We conclude that the proposed algorithm is effective to identify the PQE with an accuracy of 98.58% in a noise-free environment and 97.62% in the presence of 20 dB SNR (signal-to-noise ratio) noise. Ten simple nature PQEs and eight combined PQ events (CPQEs) with multiplicity of two, three and four are effectively detected and categorized using the algorithm. The algorithm is also tested to detect a sag PQ event due to a line-to-ground (LG) fault incident on a practical distribution utility network. The performance of the investigated method is compared with a DWT-based technique in terms of accuracy of classification with and without noise, maximum computational time of PQ detection and multiplicity of PQE which can be effectively detected. A simulation is performed using the MATLAB software. MATLAB codes are used for modelling the PQE disturbances and the proposed algorithm using mathematical formulations.

Keywords: discrete wavelet transform; distribution system; Hilbert transform; power quality event; rule-based decision tree; Stockwell transform



Citation: Singh, S.; Sharma, A.; Garg, A.R.; Mahela, O.P.; Khan, B.; Boulkaibet, I.; Neji, B.; Ali, A.; Brito Ballester, J. Power Quality Detection and Categorization Algorithm Actuated by Multiple Signal Processing Techniques and Rule-Based Decision Tree. *Sustainability* **2023**, *15*, 4317. <https://doi.org/10.3390/su15054317>

Academic Editors: Thanikanti Sudhakar Babu and Hussein A Kazem

Received: 14 December 2022

Revised: 26 January 2023

Accepted: 16 February 2023

Published: 28 February 2023



Copyright: © 2023 by the authors. Licensee MDPI, Basel, Switzerland. This article is an open access article distributed under the terms and conditions of the Creative Commons Attribution (CC BY) license (<https://creativecommons.org/licenses/by/4.0/>).

1. Introduction

Power quality (PQ) has emerged as a great challenge for power system operators. The PQ events (PQE) originate due to small and predictable changes, or large magnitude sudden changes occur on the electric grid. Recent development of consumer-electronics-driven use of electrical power introduces unprecedented challenges for the electrical grid functions. The electronics-driven consumer devices act as nonlinear loads and inject harmonic currents into the network of the electrical grid and cause PQEs, such as flicker, abrupt voltage changes, transients, and harmonics. Increased penetration of renewable energy sources (RES) into the network of the electrical grid generates PQEs [1]. PQ problems may lead to a malfunction of power system equipment, create serious disruption in the paper and semiconductor industry, and cause malfunctioning in industries such as computer, telecommunication, electronics manufacturing, pharmaceutical and data processing centers. This causes high financial loss and technical bottlenecks [2]. Hence, PQ disturbances need to be detected and classified accurately so that necessary mitigation actions may be initiated. Signal processing techniques and intelligent methods play important roles to achieve this objective. Critical analysis and comparative study of different techniques for detection and categorization of PQEs is reported in [3]. In [4] where the authors discussed a wide review of signal processing and soft computing techniques implemented for detection and categorization of causes of PQ events. A comparative study of the existing methods available in the literature is compiled. Further, major concerns and obstacles of the existing techniques for categorization of PQEs are examined and discussed in detail. In [5], the authors introduced a hybrid demodulation technique and harmonic analysis for detection and categorization of single PQEs and combined PQ events (CPQEs). A MUSIC harmonics algorithm is implemented for detection of various harmonic components. Transient, sag, swell harmonics and their combinations are effectively recognized in real time. Performance of the technique is good for recognition of the PQ disturbances of single stage and multiple stages as well. However, performance is degraded for PQ events having three or more stages. In [6], the authors designed a discrete wavelet transform (DWT) and fast Fourier transform (FFT) integrated technique to detect and classify the PQEs. DWT coefficients are used for calculating the average energy entropy of squared detailed coefficients which is used to initially detect and classify PQEs in four categories related to sag, swell, interruption and harmonics. FFT-based features are used for further classification of PQEs in each group. The classifier is effective to achieve 99.043% classification accuracy. However, performance of the method is degraded in the presence of noise. Accuracy becomes as low as 90% in the presence of noise at 20 dB SNR. In [7], the authors designed an architecture named single shot PQ detection (SSPQD) for detection and categorization of PQEs which eliminated the requirement of a sliding window. Overall accuracy of 96.55% is achieved using SSPQD. This method has relatively lower accuracy of recognition of the PQ events. It is more suitable for the primary distribution but has limitations for the secondary distribution network where large number of PQ disturbances are observed. In [8], the authors designed a dual tree complex wavelet transform (DTCWT) and support vector machine (SVM)-based technique to accurately detect and classify different single-stage PQEs and CPQEs, including transient, flicker, MI, swell, sag, harmonics and their combinations. This method has limitation for detection of the single-stage PQ events and PQ events of two stages. In [9], authors designed a hybrid algorithm using DWT and ST to detect and categorize the PQEs in real-time scenarios. This method is applicable for recognition of single-stage PQ events, and performance is degraded in the presence of noise. Different techniques for detection, classification and monitoring of PQEs in real time are reported in [10–12]. In [13], the authors designed a modified ST (MST) technique for recognition of PQ events based on the use of energy concentration of a signal and the frequency interval. This method has limitations of detection of PQ disturbances which involve the voltage magnitude change and transient components. In [14], the authors designed a sequential and multivariate method for real-time detection and classification of PQ disturbances in power delivery systems. This method has limitations of detecting the PQ events with more than five cycles.

Accuracy of the method is decreased for PQ disturbances with a time duration less than a five-cycle period. In [15], the authors designed a practical heuristic methodology for detection and classification of PQ events using empirical wavelet transform (EWT) and support vector machine (SVM) method. This is effective to detect single-stage PQ events.

After detailed and in-depth review of the algorithms and techniques discussed in the above paragraphs, we determined that existing signal-processing-based PQ identification techniques use weight factors and computational complexity on the higher side. This research gap has been considered for investigations in this paper, and the following are the main research contribution points.

- A PQ detection and categorization algorithm actuated by multiple signal processing techniques and rule-based decision tree (RBDT) is designed. This uses the processing of voltage waveform with PQE using ST, HT and DWT. RBDT is used for categorization of PQEs.
- The algorithm has the advantage of replacing the weight factor by the features computed from the PQE signal, and the computational burden is reduced. Hence, the weight factor requirement has been eliminated. The selected features effectively classify the PQEs with high accuracy and low computational time of 0.080564 s. Hence, accuracy as high as intelligent techniques was achieved using a simple nature RBDT classifier.
- The algorithm is effective to identify the PQEs with an accuracy of 98.58% in a noise-free environment and 97.62% in the presence of 20 dB SNR (signal-to-noise ratio).
- The algorithm effectively detected and categorized the ten simple nature PQEs and eight CPQEs.
- The algorithm is also tested to detect a sag PQ event due to an LG fault incident in a practical distribution utility network.
- A comparative study of the investigated method with a DWT-based technique is performed, and it is established that the investigated method performs better compared to a DWT in terms of accuracy of classification with and without noise, maximum computational time of PQ detection and multiple PQEs.

This paper includes the contents in eight different headings. Section 1 is the Introduction where a basic introduction to the research area considered for investigation, a review of the literature, research gaps, research contribution and paper structure is discussed. Mathematical formulations for generation of PQEs are discussed in Section 2. The designed algorithm actuated by multiple signal processing techniques to recognize PQEs and different mathematical formulations are elaborated on in Section 3. Simulation results for PQE detection are elaborated on in Section 4. Section 5 discussed the classification of PQEs. Validation of the PQE recognition algorithm on real-time data of a distribution utility network is included in Section 6. A performance comparative study is discussed in Section 7. Concluding remarks of the research work are included in Section 8.

2. Mathematical Formulation for Generation of PQE

A voltage signal without a power quality event (PQE) and voltage signal with a single-stage PQE are generated using the mathematical models reported in [16]. The mathematical formulations of various PQEs used for validation of the proposed method are detailed in this section. Abbreviations used in the mathematical formulations are detailed here: A: amplitude; f: frequency; V: voltage; T: time period; τ : time constant; ω : angular frequency; and $u(t)$: unit step function .

1. Voltage waveform without PQE is modeled using the below expression.

$$V(t) = A \sin(\omega t) \quad (1)$$

2. Voltage waveform with a sag PQE is modeled using the below expression.

$$V(t) = (1 - \alpha(u(t - t_1) - u(t - t_2))) \sin(\omega t) \quad (2)$$

3. Voltage waveform with a swell PQE is modeled using the below expression.

$$V(t) = (1 + \alpha(u(t - t_1) - u(t - t_2)))\sin(\omega t) \quad (3)$$

4. Voltage waveform with a momentary interruption PQE is modeled using the below expression.

$$V(t) = (1 - \alpha(u(t - t_1) - u(t - t_2)))\sin(\omega t) \quad (4)$$

5. Voltage waveform with harmonics PQE is modeled using the below expression.

$$V(t) = \alpha_1\sin(\omega t) + \alpha_3\sin(3\omega t) + \alpha_5\sin(5\omega t) + \alpha_7\sin(7\omega t) \quad (5)$$

6. A voltage waveform with flicker PQE is modeled using the below expression.

$$V(t) = (1 + \alpha_f\sin(\beta\omega t))\sin(\omega t) \quad (6)$$

7. A voltage waveform with an oscillatory transient PQE is modeled using the below expression.

$$V(t) = \sin(\omega t) + \alpha e^{\frac{(t-t_1)}{\tau}} \sin\omega_n(t - t_1)\{u(t_2 - u(t_1))\} \quad (7)$$

8. A voltage waveform with an impulsive transient PQE is modeled using the below expression.

$$V(t) = \sin(\omega t) + \alpha e^{\frac{(t-t_1)}{\tau}} - \alpha e^{\frac{(t-t_1)}{\tau}}\{u(t_2 - u(t_1))\} \quad (8)$$

9. A voltage waveform with a notches PQE is modeled using the below expression.

$$V(t) = \sin(\omega t) - \text{sign}(\sin(\omega t)) \times \left[\sum_{n=0}^9 K \times \{u(t - (t_1 + 0.02n)) - u(t - (t_2 + 0.02n))\} \right] \quad (9)$$

10. A voltage waveform with a spikes PQE is modeled using the below expression.

$$V(t) = \sin(\omega t) + \text{sign}(\sin(\omega t)) \times \left[\sum_{n=0}^9 K \times \{u(t - (t_1 + 0.02n)) - u(t - (t_2 + 0.02n))\} \right] \quad (10)$$

PQEs with multiplicities of two, three and four are generated by a combination of PQEs modelled using the above detailed Equations (1) to (10). Parameters defined in the standards of power quality (PQ) and simulated parameters of the voltage signal with and without a PQE are detailed in Table 1. The parameters of a PQE reported in [17] are used to simulate the PQEs investigated in this paper. PQEs having multiplicity two, multiplicity three and multiplicity four are simulated by hybridization of the mathematical models described in Table 1.

Table 1. Standard and simulated parameters of PQEs.

Power Quality Event	PQE Parameters	
	Standard	Simulated
Voltage waveform without PQE	$\omega = 2\pi f$	$A = 1pu, f = 50 \text{ Hz}$
Voltage sag PQE	$0.1 \leq \alpha \leq 0.9, T \leq t_2 - t_1 \leq 9T$	$\alpha = 0.3, t_1 = 0.06, t_2 = 0.14$
Voltage swell PQE	$0.1 \leq \alpha \leq 0.8, T \leq t_2 - t_1 \leq 9T$	$\alpha = 0.3, t_1 = 0.06, t_2 = 0.14$
Voltage Momentary interruption PQE	$0.9 \leq \alpha \leq 1.0, T \leq t_2 - t_1 \leq 9T$	$\alpha = 0.95, t_1 = 0.06, t_2 = 0.14$
Voltage harmonics PQE	$0.1 \leq \alpha_3, \alpha_5, \alpha_7 \leq 0.15$	$\alpha_3 = 0.05, \alpha_5 = 0.10, \alpha_7 = 0.15$
Voltage flicker PQE	$0.1 \leq \alpha_f \leq 0.2, 5 \leq \beta \leq 20 \text{ Hz}$	$\alpha_f = 0.15, \beta = 15$
Oscillatory transient PQE	$0.1 \leq \alpha \leq 0.8, 0.05T \leq t_2 - t_1 \leq 3T, 8 \text{ ms} \leq \tau \leq 40 \text{ ms}, 300 \leq f_n \leq 900 \text{ Hz}$	$\alpha = 0.8, t_1 = 0.08, \tau = 0.02, t_2 = 0.10$
Impulsive transient PQE	$1 \leq \alpha \leq 10, 0.05T \leq t_2 - t_1 \leq 3T, 8 \text{ ms} \leq \tau \leq 40 \text{ ms}$	$\alpha = 10, t_1 = 0.085, \tau = 0.02, t_2 = 0.088$
Voltage notches PQE	$0.1 \leq K \leq 0.4, 0 \leq t_1, t_2 \leq 0.5T, 0.01T \leq t_2 - t_1 \leq 0.05T$	$K = 0.4, t_1 = 0.006, t_2 = 0.0065$
Voltage spikes PQE	$0.1 \leq K \leq 0.4, 0 \leq t_1, t_2 \leq 0.5T, 0.01T \leq t_2 - t_1 \leq 0.05T$	$K = 0.4, t_1 = 0.002, t_2 = 0.0023$

3. Algorithm Actuated by Multiple Signal Processing Techniques to Recognize PQE

This section details the various steps of the algorithm actuated by multiple signal processing techniques and used to recognize power quality events (PQE). All steps of the algorithm are depicted in Figure 1. Steps for detection and classification of various PQEs are elaborated in the subsections below.

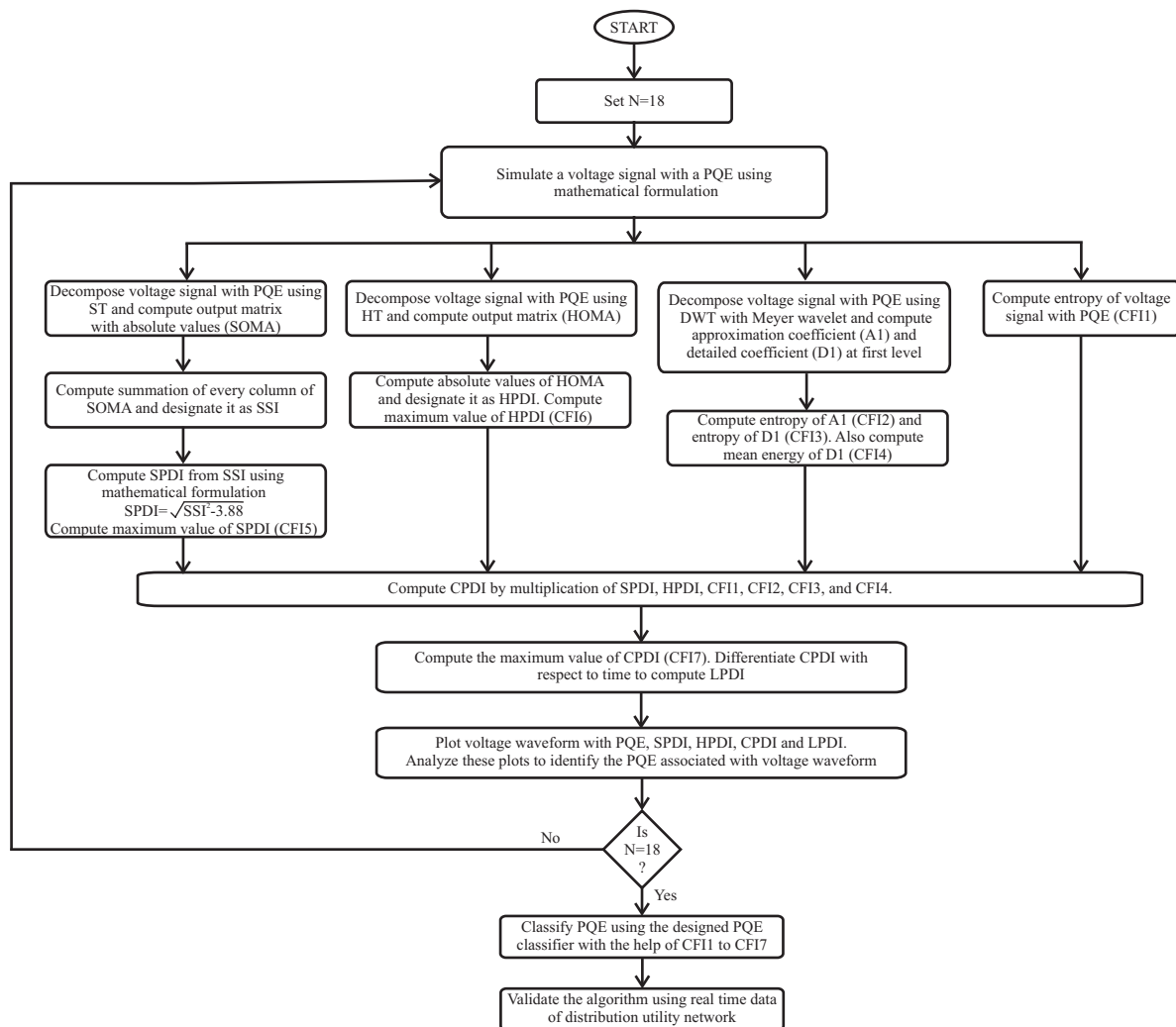


Figure 1. PQ recognition algorithm actuated by multiple signal processing techniques.

3.1. Detection of PQE

The computation of the Stockwell PQ detection index (SPDI), the Hilbert PQ detection index (HPDI), the combined PQ detection index (CPDI) and the combined feature index (CFI) is discussed in this section.

3.1.1. Stockwell PQ Detection Index

A voltage signal ($v(t)$) with a PQE is decomposed by applying the Stockwell transform (ST) using the mathematical expression described below, and the Stockwell output matrix (SOM) is computed.

$$SOM(\tau, f) = \int_{-\infty}^{\infty} v(t)g(\tau - t)e^{-2\pi ft} dt \quad (11)$$

where $g(\tau)$ is the Gaussian modulation function which can be expressed by the formulation described below [18]:

$$g(\tau) = \frac{|f|}{\sqrt{2\pi}} e^{-(\tau^2/(2\sigma^2))} \quad (12)$$

where σ is defined as the reciprocal of the magnitude of the frequency as detailed below [18]. A detailed description of the ST is available in [19].

$$\sigma = \frac{1}{|f|} \quad (13)$$

The output matrix of the ST (SOM) is a complex valued matrix with the dimension 320×640 and represents the voltage signal with a PQ disturbance in a frequency domain where the signal magnitude with respect to the frequency is represented by the matrix elements. A matrix of absolute values of SOM (SOMA) is computed as detailed in the equation below.

$$SOMA = |SOM| \quad (14)$$

The Stockwell summation index (SSI) is computed by summing all elements of every column of the SOMA as detailed in the equation below. Here, m and n represent the total number of rows and column in the SOMA matrix. Further, i and j indicate the number of rows and columns for an iteration. The SSI is effective to find the maximum magnitude for a frequency component available with the signal except the fundamental frequency. For the fundamental signal frequency, the magnitude of SSI becomes zero. Therefore, SSI is effective to find the availability of frequency components other than the fundamental ones.

$$SSI = \sum_{j=1}^n \sum_{i=1}^m (SOMA) \quad (15)$$

The Stockwell PQ detection index (SPDI) is computed from SSI using the detailed mathematical expression below:

$$SPDI = \sqrt{SSI^2 - 3.88} \quad (16)$$

The SPDI transforms the SSI into a unit magnitude signal. Therefore, any change from the standard value of one per unit is effectively identified by the use of the SPDI. This effectively identifies the magnitude of all frequency components. However, performance of the SPDI is slightly deteriorated in the noisy environment.

3.1.2. Hilbert PQ Detection Index

We decompose the voltage signal with PQE ($v(t)$) using the Hilbert transform (HT) and compute the output matrix (HOM) as described below:

$$HOM = \frac{1}{\pi} PV \int_{-\infty}^{\infty} \frac{v(t)}{t - \tau} d\tau \quad (17)$$

where PV indicates the Cauchy's principle value integral. A detailed description of the HT is available in [20]. We compute the Hilbert PQ detection index (HPDI) by taking absolute values of HOM as detailed in the equation below. The output matrix of the HT (HOM) is a complex valued column matrix with the dimension 640×1 and represents the voltage signal with PQ disturbance in frequency domain.

$$HPDI = |HOM| \quad (18)$$

The HPDI is effective to detect the magnitude related disturbances effectively. Performance of the HPDI is quite high even in the noisy environment.

3.1.3. Combined PQ Detection Index

The combined PQ detection index (CPDI) is computed by multiplying the SPDI, the HPDI and classification feature indexes CFI1, CFI2, CFI3 and CFI4 element by element as detailed below:

$$CPDI = SPDI \times HPDI \times CFI1 \times CFI2 \times CFI3 \times CFI4 \quad (19)$$

CFIs are described in Section 3.3. The CPDI has the advantage that the weight factor has been eliminated. This is fast and detects PQEs with high accuracy. This is effective to detect the magnitudes of all frequencies superimposed on the signal and signal magnitude changes even in a high noise environment.

3.2. Location of PQE

The incidence of a PQE on the voltage signal is located with the help of location a PQ disturbance index (LPDI). The LPDI is obtained by differentiating the CPDI with respect to time as detailed below:

$$LPDI = \frac{d(CPDI)}{dt} \quad (20)$$

High magnitude peaks observed on the LPDI at the start of a PQE and the end of a PQE will locate the PQE on the voltage signal.

3.3. Classification of PQE

Classification of the PQE is performed by the classifier using the classification feature indexes (CFI). The classifier uses a simple rules-based decision tree (RBDT). The RBDT uses simple rules for classification of PQ events due to less computational burden and high accuracy. We decompose the voltage signal with the PQE using discrete wavelet transform (DWT) up to the first decomposition level to obtain an approximation coefficient (A1) and a detailed coefficient (D1) using the Meyer mother wavelet. The DWT is applied using the filter bank approach which is also known as multi-resolution analysis. The low pass (g) and high pass (h) filters are used to obtain high frequency and low frequency components. This is performed by dyadic decimation (down-sampling). The filters h and g generate a family of scaling $\phi(t)$ and wavelet $\psi(t)$ functions. The magnitudes of A1 and D1 are obtained by the equations detailed below.

$$A1 = \phi(t) = \sqrt{2} \sum_n h(n) \phi(2t - n) \quad (21)$$

$$D1 = \psi(t) = \sqrt{2} \sum_n g(n) \psi(2t - n) \quad (22)$$

where $g(n) = (-1)^n h(1 - n)$. The Meyer mother wavelet is used for the choices of (g) and (h). Feature indexes CFI1 to CFI4 help to adjust the magnitude changes according to the available disturbance which eliminates the additional fixed weight factors. Classification feature index (CFI1) indicates entropy of the voltage signal. Classification feature index (CFI2) indicates entropy of the approximation coefficient (A1). Classification feature index

(CFI3) indicates entropy of the detailed coefficient (D1). Classification feature index (CFI5) indicates the maximum value of the SPDI. Classification feature index (CFI6) indicates the maximum value of the HPDI. Classification feature index (CFI7) indicates the maximum value of the CPDI. Classification feature index (CFI4) indicates the mean energy of the detailed coefficient (D1) and is computed using the expression below:

$$CFI4 = \text{mean} \left(\sqrt{\Sigma(D1^2, 2)} \right) \quad (23)$$

Detailed mathematical formulations of entropy, computation of maximum values and mean values reported in [21–23] have been used in this paper to compute CFI1 to CFI7.

4. Identification of Power Quality Disturbances: Simulation Results

This section elaborates on the simulation results to identify the various PQ disturbances.

4.1. Power Quality Events of Multiplicity One

This section details the simulation results to detect the one PQE associated with a voltage signal.

4.1.1. Voltage Waveform without PQE

A voltage signal without a PQE is processed using the ST, and the SPDI is computed. This voltage signal is also processed using the HT to compute the HPDI. The voltage signal is decomposed using DWT to compute A1 and D1. Classification feature indexes CFI1, CFI2, CFI3 and CFI4 are computed from voltage signal A1, D1 and mean energy. The SPDI, HPDI, CFI1, CFI2, CFI3 and CFI4 are multiplied to compute the CPDI. The CPDI is differentiated with respect to time to compute the LPDI. Voltage signals without PQE, SPDI, HPDI, CPDI and LPDI are depicted in Figure 2a–e, respectively. The magnitude of classification features CFI1 to CFI7 for a voltage waveform without PQE is included in Table 2.

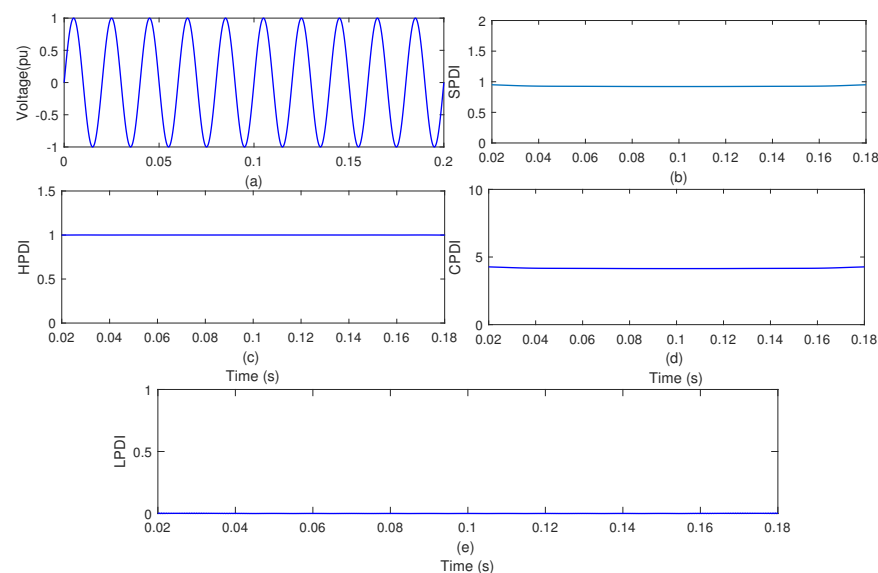


Figure 2. Voltage signal without a PQE: (a) voltage waveform; (b) SPDI; (c) HPDI; (d) CPDI; (e) LPDI.

Figure 2a shows that the pure sinusoidal nature of the waveform is maintained which indicates that PQE is not associated with the waveform. Figure 2b shows that constant magnitude of the SPDI is maintained, indicating no PQE. Figure 2c shows that constant magnitude of the HPDI is maintained, indicating no PQE. Figure 2d shows that constant magnitude of the CPDI is maintained, indicating no PQE. Figure 2e illustrates that zero

magnitude of the LPDI is maintained, indicating that a PQE is not detected and localized. The plots of Figure 2 are taken as reference plots to detect PQEs associated with a voltage signal.

Table 2. Magnitude of PQ classification indexes.

S. No.	Name of PQE	Symbol of PQE	PQE Classification Index						
			CFI1	CFI2	CFI3	CFI4	CFI5	CFI6	CFI7
1	Voltage waveform without PQE	PQE1	123.5907	115.8079	0.0095	0.0331	3.8878	1.0031	15.7912
2	Sag PQE	PQE2	143.1195	50.9959	0.0103	0.0341	3.9215	1.0270	9.0009
3	Swell PQE	PQE3	44.1925	256.4699	0.0103	0.0341	3.9177	1.3301	14.1702
4	Momentary interruption PQE	PQE4	76.1953	74.6326	0.0158	0.0421	4.0008	1.0853	13.4211
5	Harmonics PQE	PQE5	145.5911	99.5448	0.0597	0.0954	9.4477	1.3038	905.9688
6	Flicker PQE	PQE6	114.1932	128.6808	2.2121	0.6238	6.9438	1.1500	1.6179×10^5
7	Oscillatory transient PQE	PQE7	10.8656	277.8975	0.5600	0.3928	53.1015	3.2148	9.8255×10^4
8	Impulsive transient PQE	PQE8	28.8203	234.0183	0.3214	1.1774	69.9567	4.3504	7.7685×10^5
9	Voltage notch	PQE9	127.9847	96.6030	5.9705	1.2957	14.7474	1.1023	1.4724×10^6
10	Voltage spike PQE	PQE10	119.2040	122.4091	2.5074	0.9826	14.8298	1.2967	6.9136×10^5
11	Voltage sag with harmonics CPQE	CPQE1	162.1978	35.8284	0.0648	0.0981	9.4800	1.3281	404.3306
12	Voltage flicker and harmonics CPQE	CPQE2	136.0770	111.9760	2.8852	0.7069	10.1926	1.3038	3.7303×10^5
13	Voltage sag and oscillatory transient CPQE	CPQE3	25.5122	229.2883	0.5608	0.3929	53.1434	3.2031	1.9014×10^5
14	Voltage harmonics and oscillatory transient CPQE	CPQE4	30.0579	263.3202	0.6103	0.4029	51.5163	3.0888	2.6814×10^5
15	Voltage sag and impulsive transient CPQE	CPQE5	43.4669	185.4091	0.3222	1.1774	69.9575	4.3555	9.3167×10^5
16	Voltage sag and spikes CPQE	CPQE6	140.1730	55.9236	2.5079	0.9827	14.8907	1.2921	3.7120×10^5
17	Voltage sag, harmonics and oscillatory transient CPQE	CPQE7	43.5686	215.7930	0.6111	0.4029	51.5582	3.0772	3.1810×10^5
18	Voltage sag, harmonics, impulsive transient and oscillatory transient CPQE	CPQE8	61.4301	350.0827	1.4546	0.7718	51.6290	3.5917	3.6595×10^6

4.1.2. Voltage Sag PQE

A voltage signal with a sag PQE is processed using the proposed PQ recognition method to compute SPDI, HPDI, CPDI, LPDI and CFIs. Voltage signals with sag PQE, SPDI, HPDI, CPDI and LPDI are depicted in Figure 3a–e, respectively. The magnitude of classification features CFI1 to CFI7 for a voltage waveform with a sag PQE is included in Table 2.

Figure 3a shows that the magnitude of the voltage waveform is decreased between 0.06 s and 0.14 s which indicates that a sag PQE is associated with the waveform. Figure 3b shows that magnitude of the SPDI is decreased between 0.06 s and 0.14 s which indicates that a sag PQE is detected. Further, peaks observed at 0.06 s to 0.14 s indicate the starting and end of the sag PQE. Figure 3c shows that magnitude of the HPDI is decreased between 0.06 s and 0.14 s which indicates that a sag PQE is detected. Figure 3d shows that the magnitude of the CPDI is decreased between 0.06 s and 0.14 s which indicates that a sag PQE is detected. Further, peaks observed at 0.06 s to 0.14 s indicate the starting and the end of a sag PQE. Figure 3e shows that the high magnitude of the LPDI at 0.06 s to 0.14 s helps to localize the sag PQE with respect to time.

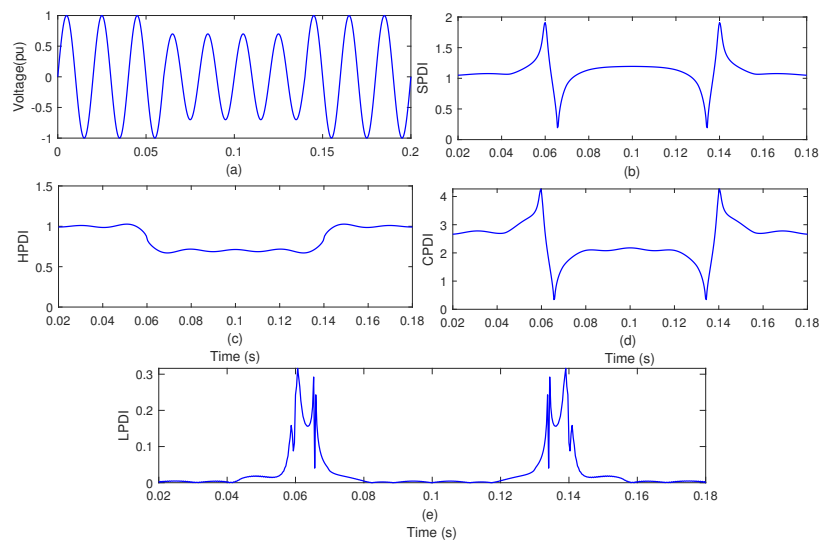


Figure 3. Voltage sag PQE: (a) voltage waveform; (b) SPDI; (c) HPDI; (d) CPDI; (e) LPDI.

4.1.3. Voltage Swell PQE

A voltage signal with a swell PQE is processed using the ST, and the SPDI is computed. This voltage signal is also processed using the HT to compute the HPDI. The voltage signal with a sag PQE is decomposed using a DWT, and coefficients A1 and D1 are computed. Classification feature indexes CFI1, CFI2, CFI3 and CFI4 are computed from the voltage signal with a swell PQE, A1, D1 and mean energy. The SPDI, HPDI, CFI1, CFI2, CFI3 and CFI4 are multiplied to compute the CPDI. The CPDI is differentiated with respect to time to compute the LPDI. The voltage signal with a swell PQE, SPDI, HPDI, CPDI and LPDI are depicted in Figure 4a–e, respectively. The magnitude of the classification features CFI1 to CFI7 for the voltage waveform with a swell PQE is included in Table 2.

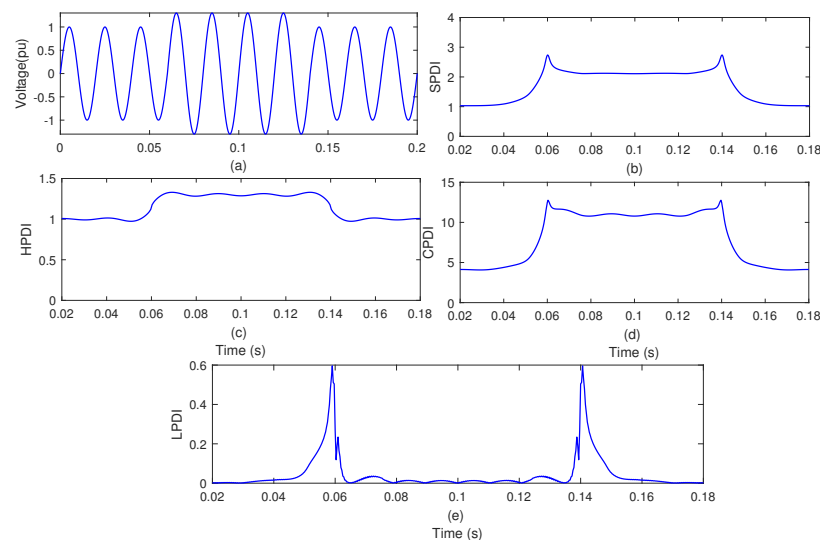


Figure 4. Voltage swell PQE: (a) voltage waveform; (b) SPDI; (c) HPDI; (d) CPDI; (e) LPDI.

Figure 4a shows that the increased magnitude of voltage from 0.06 s to 0.14 s time indicates a swell PQE. Figure 4b shows that the magnitude of the SPDI is increased between 0.06 s and 0.14 s which indicates the presence of a swell PQE. Further, peaks observed at 0.06 s to 0.14 s indicate the starting and end of the swell PQE. Figure 4c shows that increased magnitude of the HPDI between 0.06 s and 0.14 s indicates a swell PQE. Figure 4d shows that the magnitude of the CPDI is increased between 0.06 s and 0.14 s which indicates a swell PQE. Further, small magnitude peaks observed at 0.06 s to 0.14 s indicate the starting

and the end of a swell PQE. Figure 4e illustrates that the high magnitude of the LPDI at 0.06 s to 0.14 s localizes the swell PQE with respect to time.

A voltage swell is simulated for 10%, 20% and 30% swell magnitude and processed using the proposed algorithm to compute the CPDI and the LPDI. These are illustrated in Figure 5. Figure 5a shows that the magnitude of the CPDI is increased between 0.06 s and 0.14 s for 10%, 20% and 30% swell magnitude which effectively detects the swell PQE of different magnitude. Figure 5b shows that the high magnitude of the LPDI at 0.06 s to 0.14 s helps to localize the swell PQE with respect to time for the swell of 10%, 20% and 30% swell magnitude.

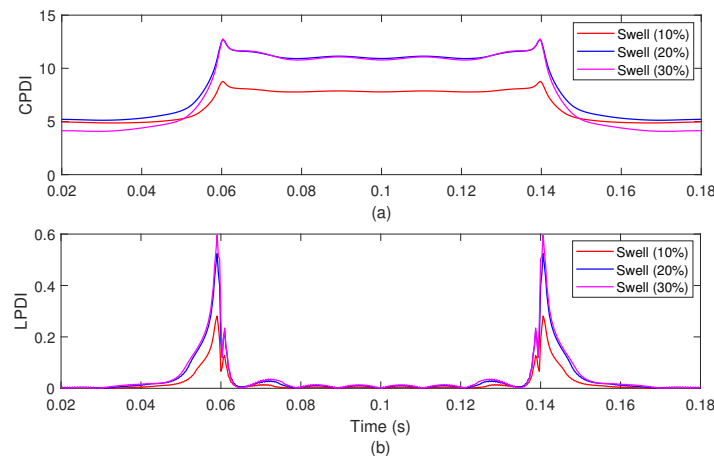


Figure 5. Voltage swell PQE with 10%, 20% and 30% swell magnitude: (a) CPDI; (b) LPDI.

4.1.4. Voltage Momentary Interruption PQE

A voltage signal with a momentary interruption (MI) PQE is processed using the ST and the HT to compute the SPDI and the HPDI, respectively. This voltage signal with MI is decomposed using DWT for computing the A1 and D1. Classification feature indexes CFI1, CFI2, CFI3 and CFI4 are computed from the voltage signal with MI, A1, D1 and mean energy. The SPDI, HPDI, CFI1, CFI2, CFI3 and CFI4 are multiplied to compute the CPDI. The CPDI is differentiated with respect to time for computing the LPDI. The voltage signal with MI PQE, SPDI, HPDI, CPDI and LPDI are illustrated in Figure 6a–e, respectively. The magnitude of classification features CFI1 to CFI7 is included in Table 2.

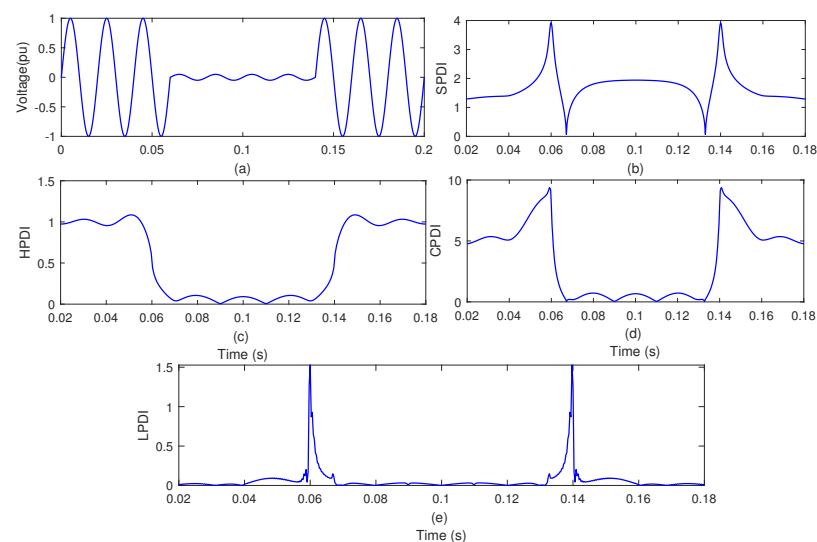


Figure 6. Voltage momentary interruption PQE: (a) voltage waveform; (b) SPDI; (c) HPDI; (d) CPDI; (e) LPDI.

Figure 6a shows that the magnitude of the voltage waveform is decreased and becomes less than 10% between 0.06 s and 0.14 s which indicates an MI. Figure 6b shows that the magnitude of the SPDI is decreased between 0.06 s and 0.14 s which indicates an MI. Further, peaks observed at 0.06 s to 0.14 s indicate the starting and end of an MI. Figure 6c shows that the magnitude of the HPDI is decreased and becomes near to zero between 0.06 s and 0.14 s which indicates an MI. Figure 6d shows that the magnitude of the CPDI is decreased and becomes near zero between 0.06 s and 0.14 s which indicates that an MI is detected. Further, peaks observed at 0.06 s to 0.14 s indicate the starting and end of an MI. Figure 6e, illustrates that the high magnitude of the LPDI at 0.06 s to 0.14 s localizes the MI with respect to time.

4.1.5. Voltage Harmonics PQE

A voltage signal with a harmonics PQE is processed using the proposed PQE recognition method to compute different indexes. The voltage signal with harmonics PQE, SPDI, HPDI, CPDI and LPDI are depicted in Figure 7a–e, respectively. The magnitudes of classification features CFI1 to CFI7 are included in Table 2.

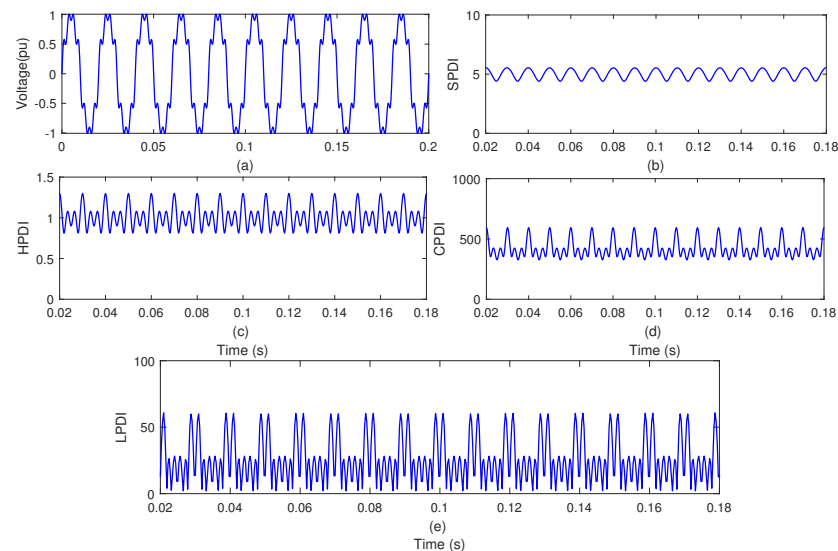


Figure 7. Voltage harmonics PQE: (a) voltage waveform; (b) SPDI; (c) HPDI; (d) CPDI; (e) LPDI.

Figure 7a shows that harmonics are associated with the voltage waveform at a regular interval. Figure 7b shows that ripples of the regular pattern are associated with the SPDI which indicates that a harmonics PQE is present. Figure 7c shows that a pattern of three ripples with one peak high and two peaks relatively low is observed over the entire time range with the HPDI which indicates the presence of harmonics. Figure 7d shows that a pattern of three ripples with one peak high and two peaks relatively low is observed over the entire time range with the CPDI which indicates the presence of harmonics. Figure 7e shows that a pattern of six ripples with two peaks high and four peaks relatively low is observed over the entire time range of the LPDI which locates the presence of every harmonic.

4.1.6. Voltage Flicker PQE

A voltage signal with a flicker PQE is processed using the ST, and the SPDI is computed. The voltage signal is also processed using the HT to compute the HPDI. The voltage signal is decomposed using DWT, and A1 and D1 are computed. Classification feature indexes CFI1, CFI2, CFI3 and CFI4 are computed from the voltage signal with flicker PQE, A1, D1 and mean energy. The SPDI, HPDI, CFI1, CFI2, CFI3 and CFI4 are multiplied to compute the CPDI. The CPDI is differentiated with respect to time to compute the LPDI. Voltage signals with flicker PQE, SPDI, HPDI, CPDI and LPDI are depicted in Figure 8a–e, respectively. The magnitude of classification features CFI1 to CFI7 for a voltage waveform with flicker PQE is included in Table 2.

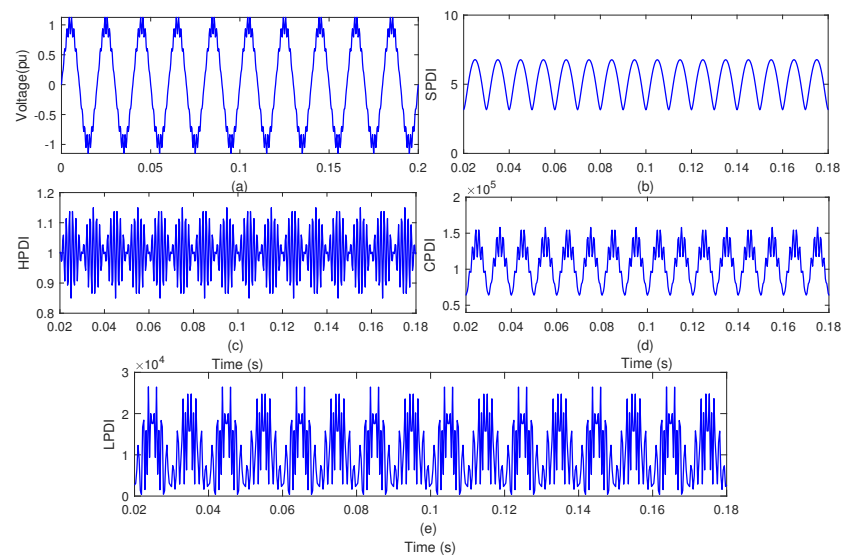


Figure 8. Voltage flicker PQE: (a) voltage waveform; (b) SPDI; (c) HPDI; (d) CPDI; (e) LPDI.

Figure 8a shows that flickers are associated with voltage waveform with every half cycle as indicated by concentrated frequency components near the peak of the waveform. Figure 8b shows that ripples of a regular pattern having a flat top and sharp trough are associated with the SPDI which indicates the flicker. Figure 8c shows that a waveform pattern having a magnitude increasing from zero to peak in both directions and then decreasing again corresponding to every half cycle of voltage waveform is observed over the entire time range with the HPDI which indicates the presence of flicker. Figure 8d shows that a pattern of ripples of regular pattern having a flat top along with concentrated frequency components near the peak and a sharp trough are associated with the CPDI which indicates the presence of flicker. Figure 8e shows that a regular pattern of positive side magnitudes which have a large number of peaks following a pattern of increasing magnitude to a high value and subsequently decreasing over the entire time range of the LPDI is observed, which indicates the presence of every component of flicker.

4.1.7. Oscillatory Transient PQE

A voltage signal with an oscillatory transient (OT) PQE is processed using the ST, and the SPDI is computed. This voltage signal with OT is processed using the HT to compute the HPDI. The voltage signal with OT is decomposed using DWT to compute A1 and D1. Classification feature indexes CFI1, CFI2, CFI3 and CFI4 are computed from the voltage signal with OT, A1, D1 and mean energy. The SPDI, HPDI, CFI1, CFI2, CFI3 and CFI4 are multiplied to compute the CPDI. The CPDI is differentiated with respect to time to compute the LPDI. Voltage signals with OT, SPDI, HPDI, CPDI and LPDI are depicted in Figure 9a–e respectively. The magnitude of classification features CFI1 to CFI7 for the voltage waveform with OT is included in Table 2.

Figure 9a shows that a high magnitude bump with large transient components is observed between 0.08 s and 0.10 s on the voltage waveform which indicates an OT. Figure 9b shows that the high magnitude of the SPDI is observed between 0.08 s and 0.10 s which indicates that an OT is present. Further, peaks are also observed at 0.08 s to 0.10 s which indicates the starting and the end of the OT. Figure 9c shows that high magnitude ripples are observed on the HPDI between 0.08 s and 0.10 s which indicates that an OT is present. Figure 9d shows that the high magnitude of the CPDI with ripples on the upper surface is observed between 0.08 s and 0.10 s which indicates that an OT is present. Figure 9e shows that high magnitude peaks are observed on the LPDI between 0.08 s and 0.10 s which helps to localize the OT with respect to time.

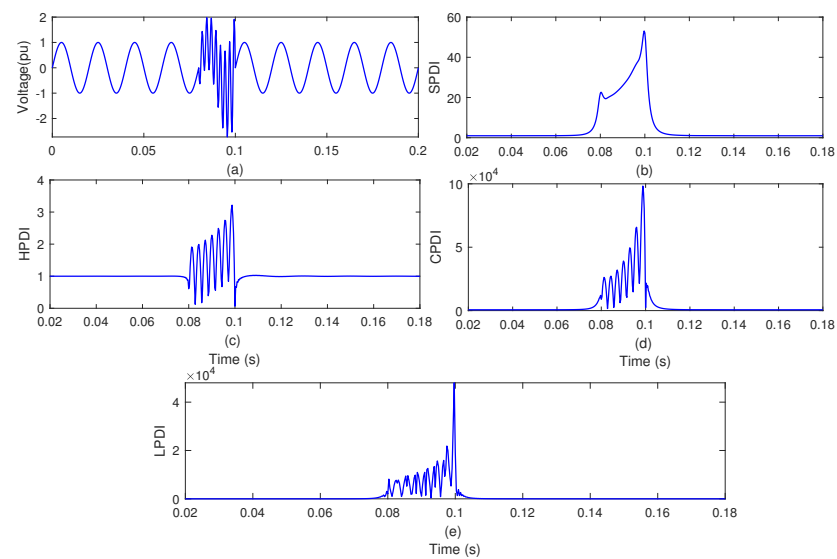


Figure 9. Voltage oscillatory transient PQE: (a) voltage waveform; (b) SPDI; (c) HPDI; (d) CPDI; (e) LPDI.

4.1.8. Impulsive Transient PQE

A voltage signal with a PQE of an impulsive transient (IT) is processed using the ST, and the SPDI is computed. This voltage signal with an IT is also processed using the HT to compute the HPDI. The voltage signal with the IT is decomposed using DWT, and coefficients A1 and D1 are computed. Classification feature indexes CFI1, CFI2, CFI3 and CFI4 are computed from the voltage signal with the IT, A1, D1 and mean energy. The SPDI, HPDI, CFI1, CFI2, CFI3 and CFI4 are multiplied to compute the CPDI. The CPDI is differentiated with respect to time to compute the LPDI. Voltage signals with the IT, SPDI, HPDI, CPDI and LPDI are depicted in Figure 10a–e, respectively. The magnitude of classification features CFI1 to CFI7 for the voltage waveform with an IT is included in Table 2.

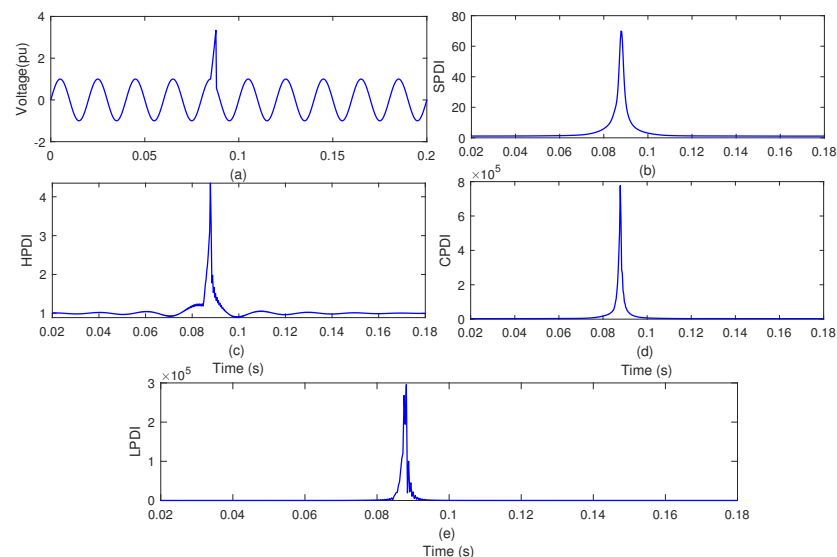


Figure 10. Voltage impulsive transient PQE: (a) voltage waveform; (b) SPDI; (c) HPDI; (d) CPDI; (e) LPDI.

Figure 10a shows that a sharp high magnitude peak is associated with the voltage waveform between 0.085 s and 0.088 s, indicating an IT. Figure 10b shows that the high magnitude sharp peak observed on the SPDI between 0.085 s and 0.088 s also indicates an IT. Figure 10c shows that a high magnitude sharp peak is observed on the HPDI between 0.085 s

and 0.088 s which also indicates an IT. Figure 10d shows that a high magnitude sharp peak available on the CPDI between 0.085 s and 0.088 s also indicates an IT. Figure 10e shows that a high magnitude with two close sharp peaks are observed on the LPDI between 0.085 s and 0.088 s which helps to localize the IT with respect to the time.

4.1.9. Voltage Notches PQE

A voltage signal with a superimposed notches PQE is processed using the proposed method, and SPDI, HPDI, CPDI, LPDI and CFIs are computed. Voltage signals with a notches PQE, SPDI, HPDI, CPDI and LPDI are illustrated in Figure 11a–e, respectively. The magnitude of classification features CFI1 to CFI7 for the voltage waveform with a notches PQE is included in Table 2.

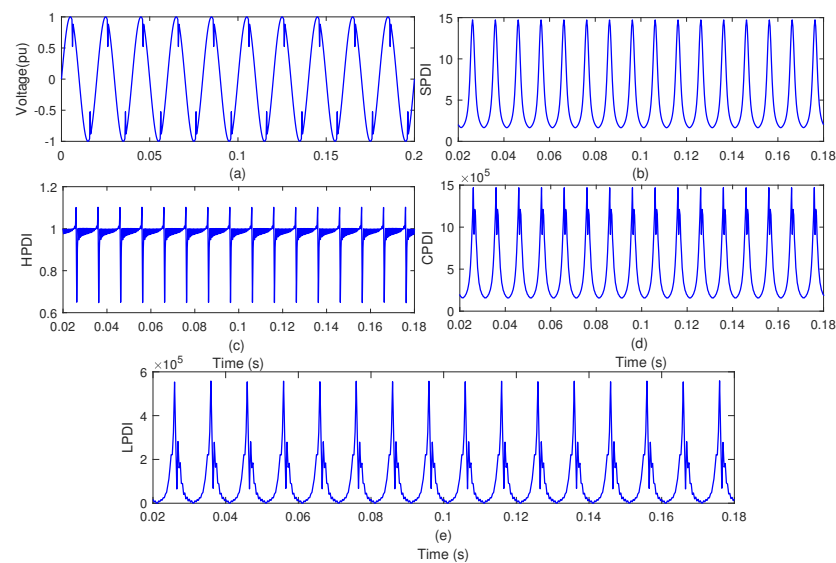


Figure 11. Voltage notches PQE: (a) voltage waveform; (b) SPDI; (c) HPDI; (d) CPDI; (e) LPDI.

Figure 11a shows that a ditch of small duration is associated with the voltage waveform for every half cycle which indicates a notch PQE. Figure 11b shows that a pattern of a high magnitude peak associated with every half cycle is observed on the SPDI which indicates that notch PQE is associated with voltage. Figure 11c shows that a pattern constituted by one high peak and one lower peak compared to base level is observed on the HPDI over the entire time range which indicates that a notches PQE is detected. Figure 11d shows that a pattern of high magnitude with two sharp close peak associated with every half cycle is observed on the SPDI which indicates that a notches PQE is associated with the waveform. Figure 11e shows that a pattern of a high magnitude peak with one peak near root level is associated with every half cycle on the LPDI which indicates that notches PQEs are localized with respect to time.

4.1.10. Voltage Spikes PQE

A voltage signal with a spikes PQE is processed using the ST, and the SPDI is computed. This voltage signal with a spikes PQE is also processed using the HT to compute the HPDI. The voltage signal with a spikes PQE is decomposed using DWT to compute A1 and D1. Classification feature indexes CFI1, CFI2, CFI3 and CFI4 are computed from a voltage signal with a spikes PQE, A1, D1 and mean energy. The SPDI, HPDI, CFI1, CFI2, CFI3 and CFI4 are multiplied to compute the CPDI. The CPDI is differentiated with respect to time to compute the LPDI. Voltage signals with a spikes PQE, SPDI, HPDI, CPDI and LPDI are depicted in Figure 12a–e, respectively. The magnitude of classification features CFI1 to CFI7 for a voltage waveform with a spikes PQE is included in Table 2.

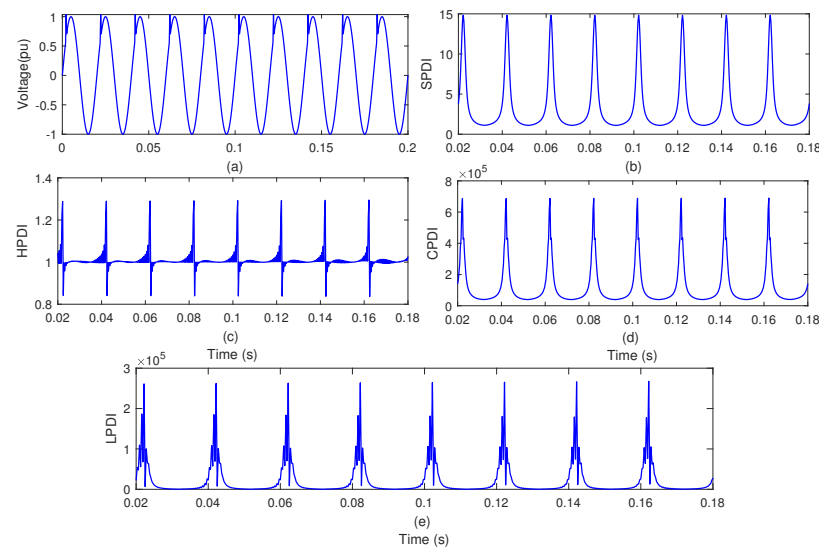


Figure 12. Voltage spikes PQE: (a) voltage waveform, (b) SPDI, (c) HPDI, (d) CPDI; (e) LPDI.

Figure 12a shows that a peak of small time interval is associated with voltage for every cycle which indicates the spikes PQE. Figure 12b shows that a pattern of a high magnitude peak associated with every cycle is observed on the SPDI which indicates that a spikes PQE is associated with voltage. Figure 12c shows that a pattern constituted by one high peak and one lower peak compared to base level is observed on the HPDI over the entire time range corresponding to every cycle which indicates that a spikes PQE is detected. Figure 12d, shows that a pattern of high magnitude with two sharp close peaks associated with every cycle is observed on the SPDI which indicates that a spikes PQE is associated with the waveform. Figure 12e shows that a pattern of a high magnitude peak with one peak near the root level is associated with every cycle on the LPDI which indicates that a spikes PQE is localized with respect to time.

4.2. Power Quality Events of Multiplicity Two

This section details the simulation results to detect two PQEs associated with a voltage signal. PQE with multiplicity two is considered a combined PQ event (CPQE).

4.2.1. Voltage Sag and Harmonics CPQE

A voltage signal with sag and harmonics CPQE is processed using the proposed PQ recognition method, and SPDI, HPDI, CPDI, LPDI and CFIs are computed. Voltage signals with sag and harmonics CPQE, SPDI, HPDI, CPDI and LPDI are depicted in Figure 13a–e, respectively. The magnitude of classification features CFI1 to CFI7 for a voltage waveform with sag and harmonics CPQE is included in Table 2.

Figure 13a shows that the magnitude of the voltage waveform is decreased between 0.06 s and 0.14 s which indicates a sag PQE. Figure 13a also shows that harmonics are associated with a voltage waveform at a regular interval. Figure 13b shows that the magnitude of the SPDI is decreased between 0.06 s and 0.14 s which indicates a sag PQE. Further, peaks observed at 0.06 s to 0.14 s indicate the starting and the end of the sag. Figure 13b also shows that ripples with a regular pattern are associated with the SPDI which indicates a harmonics PQE. Figure 13c shows that the magnitude of the HPDI is decreased between 0.06 s and 0.14 s which indicates a sag PQE. Figure 13c also shows that a pattern of three ripples with one peak high and two peaks relatively low is observed over the entire time range with the HPDI which indicates the presence of harmonics. Figure 13d shows that the magnitude of the CPDI is decreased between 0.06 s and 0.14 s which indicates that a sag PQE is detected. Further, peaks observed at 0.06 s to 0.14 s indicate the starting and the end of a sag PQE. Figure 13d also shows that a pattern of three ripples with one peak high and two peaks relatively low is observed over the entire time range with the CPDI which indicates the presence of harmonics.

Figure 13e shows that the high magnitude of the LPDI at 0.06 s to 0.14 s helps to localize the sag PQE with respect to the time. Figure 13e shows that a pattern of six ripples with two peaks high and four peaks relatively low is observed over the entire time range of the LPDI which locates the presence of every harmonic.

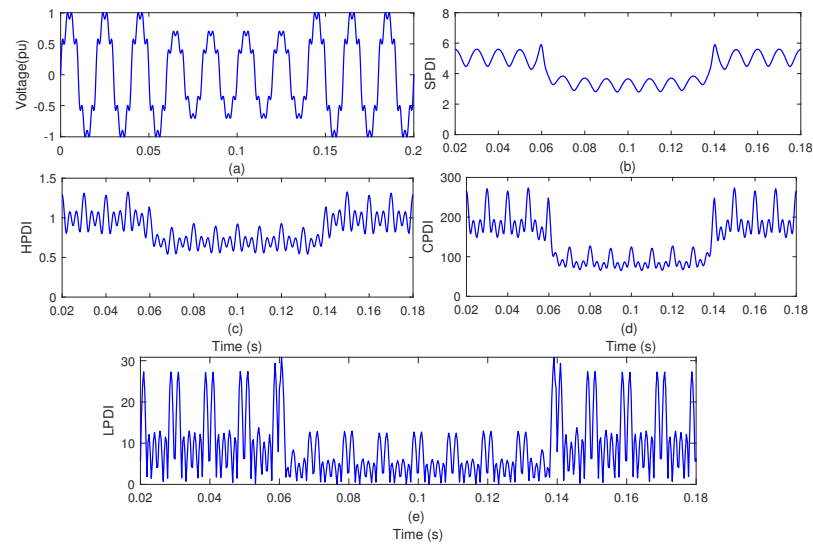


Figure 13. Voltage sag and harmonics CPQE: (a) voltage waveform; (b) SPDI; (c) HPDI; (d) CPDI, (e) LPDI.

4.2.2. Voltage Flicker and Harmonics CPQE

A voltage signal with flicker and harmonics CPQE is processed using the ST and the HT to compute the SPDI and the HPDI, respectively. The voltage signal with flicker and harmonics CPQE is decomposed using DWT to compute coefficients A1 and D1. Classification feature indexes CFI1, CFI2, CFI3 and CFI4 are computed from the voltage signal flicker and harmonics CPQE, A1, D1 and mean energy. The SPDI, HPDI, CFI1, CFI2, CFI3 and CFI4 are multiplied to compute the CPDI. The CPDI is differentiated with respect to time to compute the LPDI. Voltage signals with flicker and harmonics CPQE, SPDI, HPDI, CPDI and LPDI are depicted in Figure 14a–e, respectively. The magnitude of classification features CFI1 to CFI7 for voltage with flicker and harmonics CPQE is included in Table 2.

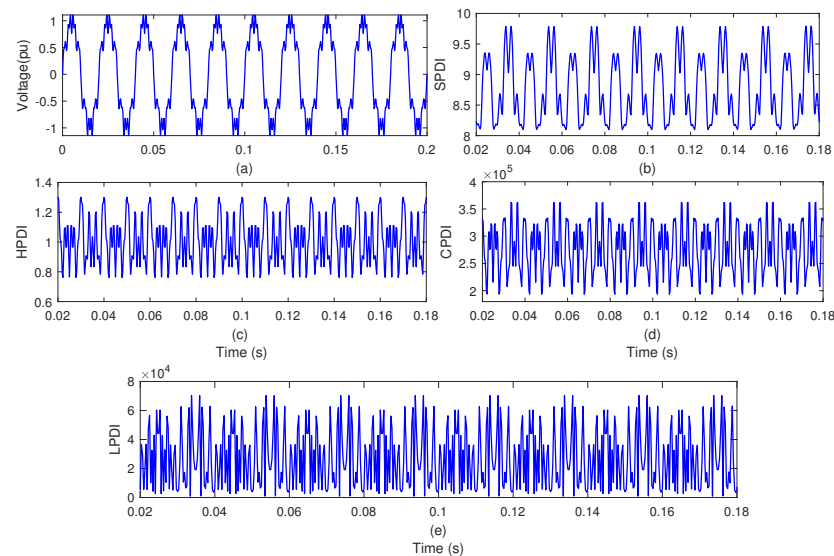


Figure 14. Voltage flicker and harmonics CPQE: (a) voltage waveform; (b) SPDI; (c) HPDI; (d) CPDI; (e) LPDI.

Figure 14a shows that flickers are associated with a voltage waveform with every half cycle as indicated by concentrated frequency components near the peak of the waveform. Figure 14b–e shows that regular pattern variations with multiple ripples on plots indicate the hybrid combination of flicker and harmonics.

4.2.3. Voltage Sag and Oscillatory Transient CPQE

A voltage signal with CPQE of sag and OT is processed using the ST and the SPDI. This voltage signal is also processed using the HT to compute the HPDI. The voltage signal with sag and OT CPQE is decomposed using DWT to compute coefficients A1 and D1. Classification feature indexes CFI1, CFI2, CFI3 and CFI4 are computed from the voltage signal with sag and OT, A1, D1 and mean energy. The SPDI, HPDI, CFI1, CFI2, CFI3 and CFI4 are multiplied to compute the CPDI. The CPDI is differentiated with respect to time to compute the LPDI. Voltage signals with sag and OT CPQE, SPDI, HPDI, CPDI and LPDI are depicted in Figure 15a–e, respectively. The magnitude of classification features CFI1 to CFI7 for the voltage waveform with sag and OT is included in Table 2.

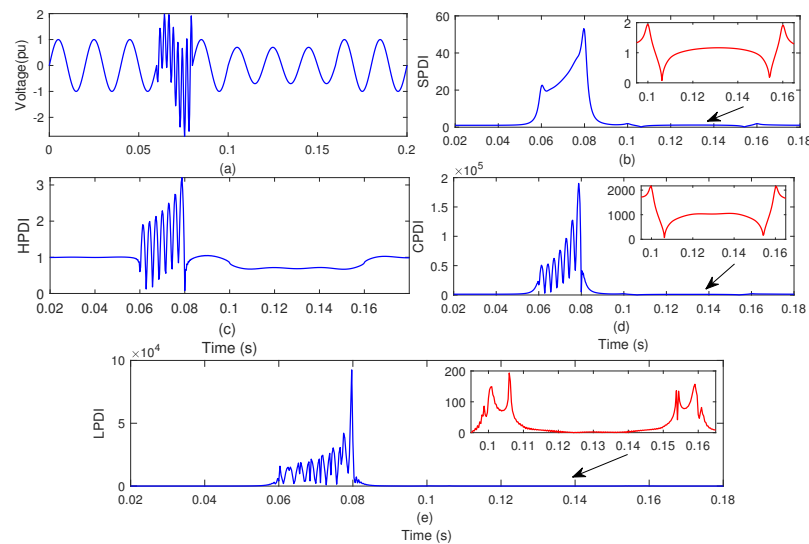


Figure 15. Voltage sag and oscillatory transient CPQE: (a) voltage waveform; (b) SPDI; (c) HPDI; (d) CPDI; (e) LPDI.

Figure 15a shows that the magnitude of the voltage waveform is decreased between 0.10 s and 0.16 s which indicates that a sag PQE is associated with the waveform. Figure 15a also shows that a high magnitude bump with large transient components is observed between 0.06 s and 0.08 s on the voltage waveform which indicates an OT associated with the voltage waveform. Figure 15b shows that the magnitude of the SPDI is decreased between 0.10 s and 0.16 s which indicates that a sag PQE is detected. Further, peaks observed at 0.06 s to 0.14 s indicate the starting and end of the sag PQE. Figure 15b also shows that a high magnitude of the SPDI is observed between 0.06 s and 0.08 s which indicates that an OT is detected. Further, peaks are also observed at 0.08 s to 0.10 s which indicates the starting and the end of the OT. Figure 15c shows that magnitude of the HPDI is decreased between 0.10 s and 0.16 s which indicates that a sag PQE is detected. Figure 15c shows that high magnitude ripples are observed on the HPDI between 0.06 s and 0.08 s which indicates an OT. Figure 15d shows that the magnitude of the CPDI is decreased between 0.10 s and 0.16 s which indicates that a sag PQE is detected. Further, peaks observed at 0.06 s to 0.14 s indicate the starting and end of a sag PQE. Figure 15d shows that the high magnitude of the CPDI with ripples on the upper surface is observed between 0.06 s and 0.08 s which indicates an OT. Figure 15e shows that the high magnitude of the LPDI at 0.10 s to 0.16 s helps to localize the sag PQE with respect to time. Figure 15e

shows that high magnitude peaks are observed on the LPDI between 0.06 s and 0.08 s which helps to localize the OT with respect to the time.

4.2.4. Voltage Harmonics and Oscillatory Transient CPQE

A voltage signal with OT and harmonics CPQE is processed using the ST, and the SPDI is computed. This voltage signal with OT and harmonics CPQE is also processed using the HT to compute the HPDI. The voltage signal with OT and harmonics CPQE is also decomposed using DWT to compute A1 and D1. Classification feature indexes CFI1, CFI2, CFI3 and CFI4 are computed from the voltage signal with OT and harmonics CPQE, A1, D1 and mean energy. The SPDI, HPDI, CFI1, CFI2, CFI3 and CFI4 are multiplied to compute the CPDI. The CPDI is differentiated with respect to time to compute the LPDI. Voltage signals with OT and harmonics CPQE, SPDI, HPDI, CPDI and LPDI are depicted in Figure 16a–e, respectively. The magnitude of classification features CFI1 to CFI7 for the voltage waveform with OT and harmonics CPQE is included in Table 2.

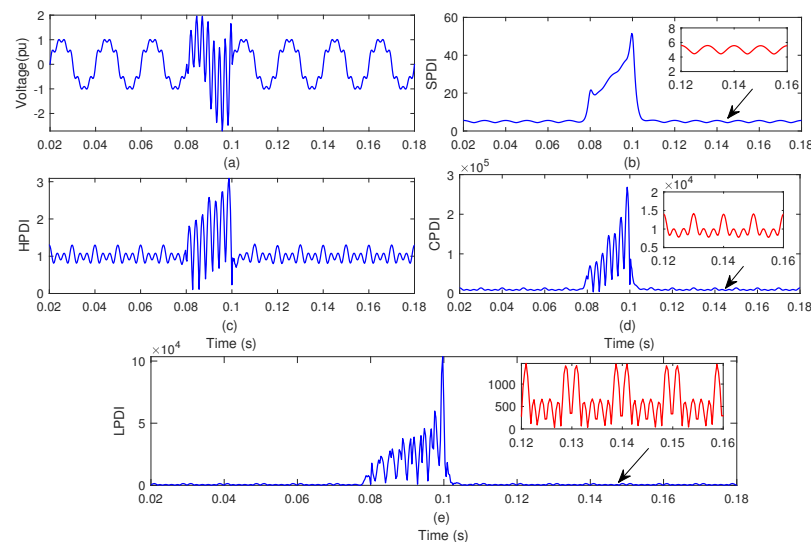


Figure 16. Voltage harmonics and oscillatory transient CPQE: (a) voltage waveform; (b) SPDI; (c) HPDI, (d) CPDI; (e) LPDI.

Figure 16a shows that harmonics are associated with the voltage waveform at a regular interval. Figure 16a also shows that a high magnitude bump with large transient components is observed between 0.08 s and 0.10 s on the voltage waveform which indicates an OT associated with the voltage waveform. Figure 16b shows that ripples with a regular pattern are associated with the SPDI which indicates that a harmonics PQE is detected. Figure 16b also shows that a high magnitude of the SPDI is observed between 0.08 s and 0.10 s which indicates an OT. Further, peaks are also observed at 0.08 s to 0.10 s which indicates the starting and the end of OT. Figure 16c shows that a pattern of three ripples with one peak high and two peaks relatively low is observed over the entire time range with the HPDI which indicates the presence of harmonics. Figure 16c also shows that high magnitude ripples are observed on the HPDI between 0.08 s and 0.10 s which indicates an OT. Figure 16d shows that a pattern of three ripples with one peak high and two peaks of relatively low magnitude are observed over the entire time range with the CPDI which indicates the presence of harmonics. Figure 16d also shows that high magnitude of the CPDI with ripples on the upper surface is observed between 0.08 s and 0.10 s which indicates an OT. Figure 16e shows that a pattern of six ripples with two peaks high and four peaks relatively low is observed over the entire time range of the LPDI which locates the presence of every harmonic. Figure 16e shows that high magnitude peaks are observed on the LPDI between 0.08 s and 0.10 s which helps to localize the OT.

4.2.5. Voltage Sag and Impulsive Transient CPQE

A voltage signal with CPQE of sag and IT is processed using the ST and the HT to compute the SPDI and the HPDI, respectively. The voltage signal with sag and IT is decomposed using DWT to compute coefficients A1 and D1. Classification feature indexes CFI1, CFI2, CFI3 and CFI4 are computed from the voltage signal sag and IT, A1, D1 and mean energy. The SPDI, HPDI, CFI1, CFI2, CFI3 and CFI4 are multiplied to compute the CPDI. The CPDI is differentiated with respect to time to compute the LPDI. Voltage signals with sag and IT, SPDI, HPDI, CPDI and LPDI are depicted in Figure 17a–e respectively. The magnitude of the classification features CFI1 to CFI7 for the voltage waveform with sag and IT CPQE is included in Table 2.

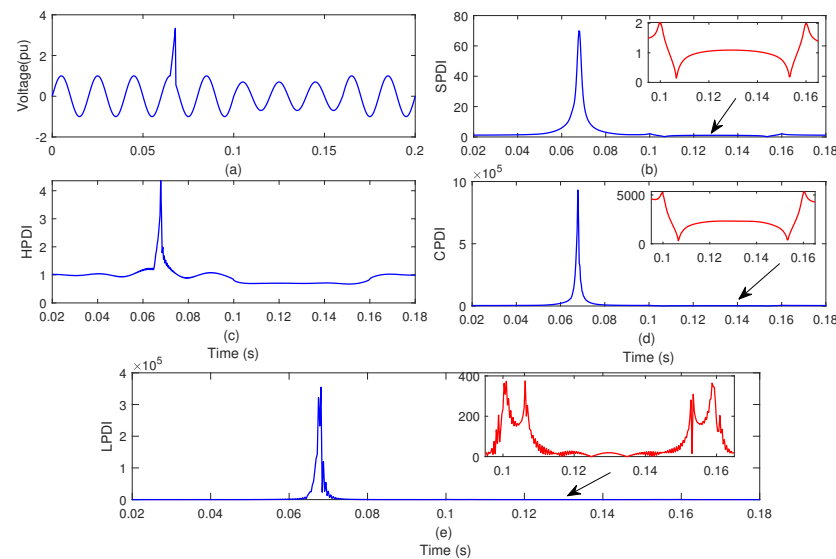


Figure 17. Voltage sag and impulsive transient CPQE: (a) voltage waveform; (b) SPDI; (c) HPDI; (d) CPDI; (e) LPDI.

Figure 17a shows that the magnitude of the voltage waveform is decreased between 0.10 s and 0.16 s which indicates a sag. Figure 17a also shows that a high magnitude sharp peak is associated with the voltage waveform between 0.085 s and 0.088 s which indicates an IT. Figure 17b shows that the magnitude of the SPDI is decreased between 0.10 s and 0.16 s which indicates a sag PQE. Further, peaks observed at 0.06 s to 0.14 s indicate the starting and the end of the sag PQE. Figure 17b also shows that the high magnitude sharp peak observed on the SPDI between 0.085 s and 0.088 s indicates an IT. Figure 17c shows that the magnitude of the HPDI is decreased between 0.10 s and 0.16 s which indicates that a sag PQE is detected. Figure 17c also shows that a high magnitude sharp peak is observed on the HPDI between 0.085 s and 0.088 s which indicates that an IT PQE is detected. Figure 17d shows that the magnitude of the CPDI is decreased between 0.10 s and 0.16 s which indicates that a sag PQE is detected. Further, peaks observed at 0.06 s to 0.14 s indicates the starting and the end of the sag PQE. Figure 17d also shows that the high magnitude sharp peak observed on the CPDI between 0.085 s to 0.088 s indicates that an IT PQE is detected. Figure 17e shows that the high magnitude of the LPDI at 0.10 s to 0.16 s helps to localize the sag PQE with respect to the time. Figure 17e shows that a high magnitude with two close sharp peaks are observed on the LPDI between 0.085 s and 0.088 s which helps to localize the IT with respect to the time.

4.2.6. Voltage Sag and Spike CPQE

A voltage signal with sag and spike CPQE is processed using the ST, and the SPDI is computed. This voltage signal with sag and spike CPQE is also processed using the HT to compute the HPDI. The voltage signal with sag and spike CPQE is decomposed using DWT to compute coefficients A1 and D1. Classification feature indexes CFI1, CFI2, CFI3 and CFI4

are computed from the voltage signal with sag and spike CPQE, A1, D1 and mean energy. The SPDI, HPDI, CFI1, CFI2, CFI3 and CFI4 are multiplied to compute the CPDI. The CPDI is differentiated with respect to time to compute the LPDI. Voltage signals with sag and spike CPQE, SPDI, HPDI, CPDI and LPDI are depicted in Figure 18a–e, respectively. The magnitude of the classification features CFI1 to CFI7 for the voltage waveform with sag and spikes CPQE is included in Table 2.

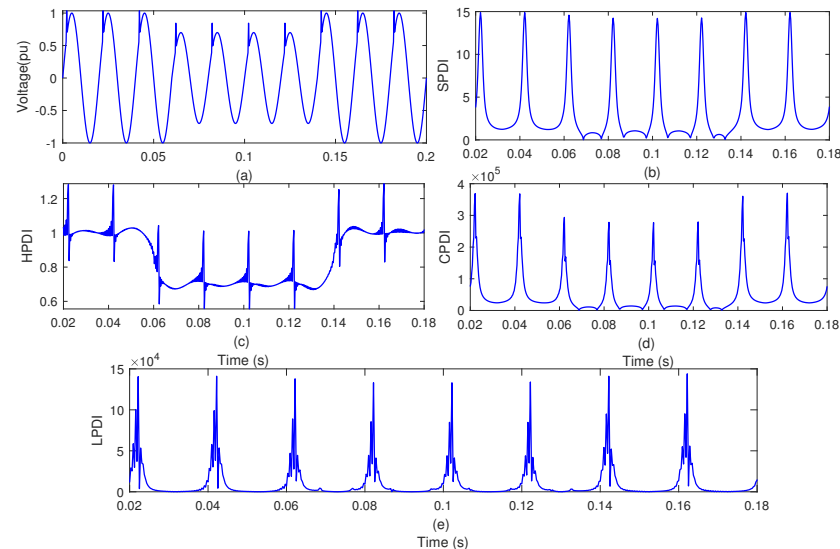


Figure 18. Voltage sag and spikes CPQE: (a) voltage waveform; (b) SPDI; (c) HPDI; (d) CPDI; (e) LPDI.

Figure 18a shows that the magnitude of the voltage waveform is decreased between 0.06 s and 0.14 s which indicates that a sag PQE is associated with the waveform. Figure 18a also shows that a peak of small duration is associated with the voltage waveform for every cycle which indicates the spikes. Figure 18b shows that the magnitude of the SPDI is decreased between 0.06 s to 0.14 s which indicates a sag. Further, peaks observed at 0.06 s and 0.14 s indicate the starting and the end of sag. Figure 18b also shows that a pattern of a high magnitude peak associated with every cycle is observed on the SPDI which indicates the spikes PQE. Figure 18c shows that the magnitude of the HPDI is decreased between 0.06 s and 0.14 s which indicates a sag PQE. Figure 18c also shows that a pattern constituted by one high peak and one lower peak compared to the base level is observed on the HPDI over the entire time range corresponding to every cycle which indicates the spikes. Figure 18d shows that the magnitude of the CPDI is decreased between 0.06 s and 0.14 s which indicates a sag PQE. Further, peaks observed at 0.06 s and 0.14 s indicate the starting and end of a sag PQE. Figure 18d also shows that a pattern of high magnitude two sharp close peaks associated with every cycle is observed on the SPDI which indicates the spikes PQE. Figure 18e shows that the high magnitude of the LPDI at 0.06 s and 0.14 s helps to localize the sag PQE. Figure 18e also shows that a pattern of high magnitude peak with one peak near the root level is associated with every cycle on the LPDI which indicates that the spikes PQE is localized.

4.3. Power Quality Events of Multiplicity Three

This section details the simulation results to detect the three PQEs associated with a voltage signal. A PQE with multiplicity three is considered a combined PQ event (CPQE).

Voltage Sag, Harmonics and Oscillatory Transient CPQE

A PQE with multiplicity three is considered a combined PQ event (CPQE). A voltage signal with CPQE of sag, harmonics and OT is processed using the ST and the HT to compute the SPDI and the HPDI, respectively. This voltage signal is decomposed using

DWT to compute coefficients A1 and D1. Classification feature indexes CFI1, CFI2, CFI3 and CFI4 are computed from a voltage signal with sag, harmonics and OT, A1, D1 and mean energy. The SPDI, HPDI, CFI1, CFI2, CFI3 and CFI4 are multiplied to compute the CPDI. The CPDI is differentiated with respect to time to compute the LPDI. Voltage signals with sag, harmonics and OT, SPDI, HPDI, CPDI and LPDI are depicted in Figure 19a–e, respectively. The magnitude of classification features CFI1 to CFI7 for a voltage waveform with sag, harmonics and OT CPQE is included in Table 2.

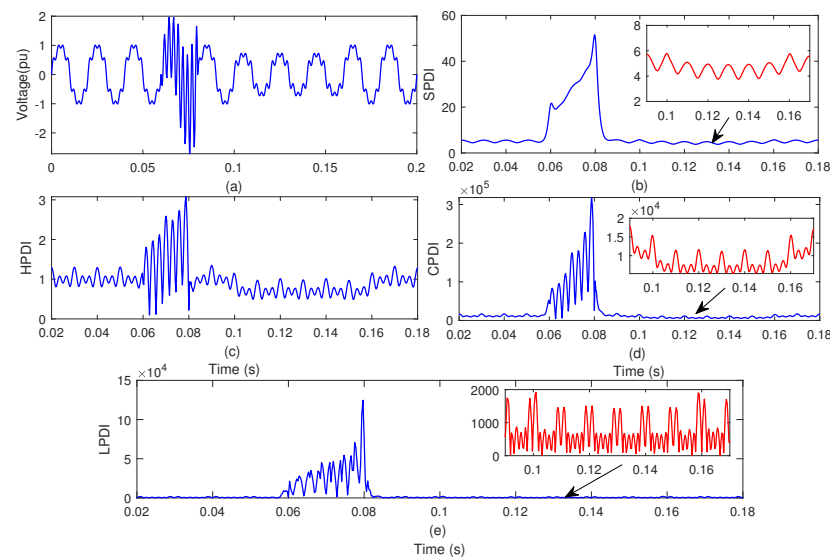


Figure 19. Voltage sag, harmonics and oscillatory transient CPQE: (a) voltage waveform; (b) SPDI; (c) HPDI; (d) CPDI, (e) LPDI.

Figure 19a shows that the magnitude of the voltage waveform is decreased between 0.10 s and 0.16 s which indicates a sag PQE. Figure 19a also shows that a high magnitude bump with large transient components is observed between 0.06 s and 0.08 s on the voltage waveform which indicates an OT. Figure 19a shows that harmonics are associated with the voltage waveform at a regular interval. Figure 19b shows that the magnitude of the SPDI is decreased between 0.10 s and 0.16 s which indicates a sag PQE. Further, peaks observed at 0.06 s and 0.14 s indicate the starting and the end of the sag PQE. Figure 19b also shows that the high magnitude of the SPDI is observed between 0.06 s and 0.08 s which indicates that an OT PQE is detected. Further, peaks are also observed at 0.08 s and 0.10 s which indicates the starting and the end of OT. Figure 19b shows that ripples with a regular pattern are associated with the SPDI which indicates that a harmonics PQE is detected. Figure 19c shows that the magnitude of the HPDI is decreased between 0.10 s and 0.16 s which indicates a sag PQE. Figure 19c shows that high magnitude ripples are observed on the HPDI between 0.06 s and 0.08 s which indicates that an OT PQE is detected. Figure 19c shows that a pattern of three ripples with one peak high and two peaks having relatively low magnitude are observed over the entire time range with the HPDI which indicates the presence of harmonics. Figure 19d shows that the magnitude of the CPDI is decreased between 0.10 s and 0.16 s which indicates a sag PQE. Further, peaks observed at 0.06 s and 0.14 s indicate the starting and the end of a sag PQE. Figure 19d shows that the high magnitude of the CPDI with ripples on the upper surface is observed between 0.06 s and 0.08 s which indicates an OT. Figure 19d shows that a pattern of three ripples with one peak high and two peaks relatively low are observed over the entire time range with the CPDI which indicates the presence of harmonics. Figure 19e shows that the high magnitude of the LPDI at 0.10 s and 0.16 s helps to localize the sag PQE. Figure 19e shows that high magnitude peaks are observed on the LPDI between 0.06 s and 0.08 s which helps to localize the OT. Figure 19e shows that a pattern of six ripples with two peaks high and

four peaks relatively low is observed over the entire time range of the LPDI which locates the presence of every harmonic.

4.4. Power Quality Events of Multiplicity Four

This section details the simulation results to detect the four PQEs associated with a voltage signal. A PQE with multiplicity four is considered a CPQE.

Voltage Sag, Harmonics, Impulsive Transient and Oscillatory Transient CPQE

A voltage signal with a CPQE of sag, harmonics, IT and OT is processed using the proposed method to compute SPDI, HPDI, CPDI, LPDI and CFIs. The voltage signal with CPQE of sag, harmonics, IT and OT, SPDI, HPDI, CPDI and LPDI are depicted in Figure 20a–e, respectively. The magnitude of the classification features CFI1 to CFI7 for the voltage waveform with sag, harmonics, IT and OT is included in Table 2.

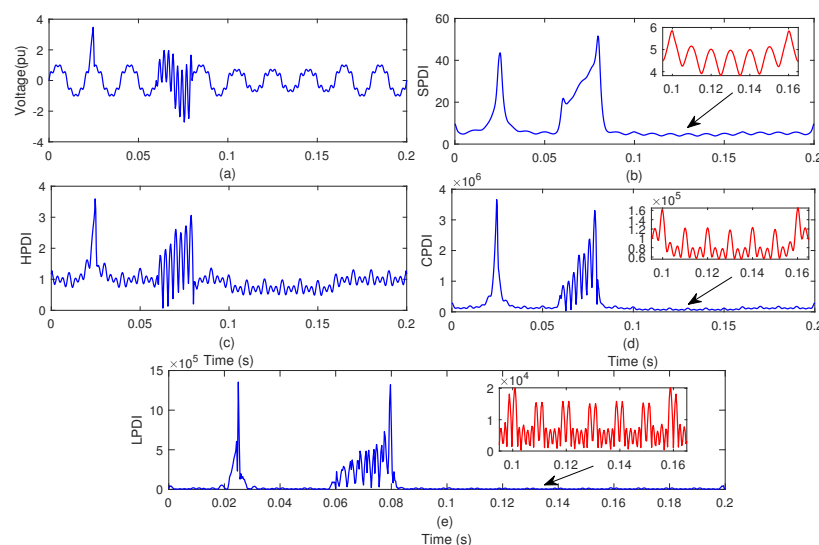


Figure 20. Voltage sag, harmonics, impulsive transient and oscillatory transient CPQE: (a) voltage waveform; (b) SPDI; (c) HPDI; (d) CPDI; (e) LPDI.

Figure 20a shows that the magnitude of the voltage waveform is decreased between 0.10 s to 0.16 s which indicates that a sag PQE is associated with the waveform. Figure 20a also shows that a high magnitude bump with large transient components is observed between 0.06 s and 0.08 s on the voltage waveform which indicates an OT associated with the voltage waveform. Figure 20a shows that harmonics are associated with the voltage waveform at a regular interval. Figure 20a shows that a high magnitude sharp peak is associated with the voltage waveform between 0.022 s and 0.025 s which indicates an IT. Figure 20b shows that the magnitude of the SPDI is decreased between 0.10 s and 0.16 s which indicates that a sag PQE is detected. Further, peaks observed at 0.06 s and 0.14 s indicate the starting and the end of the sag PQE. Figure 20b also shows that a high magnitude of the SPDI is observed between 0.06 s and 0.08 s which indicates that an OT PQE is detected. Further, peaks are also observed at 0.08 s and 0.10 s which indicates the starting and end of an OT PQE. Figure 20b shows that ripples with a regular pattern are associated with the SPDI which indicates that a harmonics PQE is detected. Figure 20b shows that the high magnitude sharp peak observed on the SPDI between 0.022 s and 0.025 s indicates that an IT is detected. Figure 20c shows that the magnitude of the HPDI is decreased between 0.10 s and 0.16 s which indicates that a sag PQE is detected. Figure 20c shows that high magnitude ripples are observed on the HPDI between 0.06 s and 0.08 s which indicates that an OT is detected. Figure 20c shows that a pattern of three ripples with one peak high and two peaks relatively low is observed over the entire time range with the HPDI which indicates the presence of harmonics. Figure 20c shows that a high magnitude

sharp peak is observed on the HPDI between 0.022 s and 0.025 s which indicates that an IT is detected. Figure 20d shows that the magnitude of the CPDI is decreased between 0.10 s and 0.16 s which indicates that a sag PQE is detected. Further, peaks observed at 0.06 s and 0.14 s indicates the starting and the end of the sag PQE. Figure 20d shows that the high magnitude of the CPDI with ripples on the upper surface is observed between 0.06 s and 0.08 s which indicates an OT. Figure 20d shows that a pattern of three ripples with one peak high and two peaks relatively low is observed over the entire time range with the CPDI which indicates the presence of harmonics. Figure 20d shows that the high magnitude sharp peak observed on the CPDI between 0.022 s and 0.025 s indicates that an IT PQE is detected. Figure 20e shows that the high magnitude of the LPDI at 0.10 s to 0.16 s helps to localize the sag PQE with respect to the time. Figure 20e shows that the high magnitude peaks are observed on the LPDI between 0.06 s to 0.08 s which helps to localize the OT with respect to the time. Figure 20e shows that a pattern of six ripples with two peaks high and four peaks relatively low is observed over the entire time range of the LPDI which locates the presence of every harmonic. Figure 20e shows that a high magnitude with two close sharp peaks are observed on the LPDI between 0.022 s and 0.025 s which helps to localize the IT.

5. Classification of PQE

The power quality events are categorized and identified using the rule-based decision tree (RBDT) using the PQE classification feature indexes CFI1 to CFI7 as features for decision rules. The decision rules and classification tree for the investigated PQEs obtained using these rules are illustrated in Figure 21. RBDT is selected for classification of the PQEs because it has a simple nature, and it is based on the use of if then else rules. This results in less computation time for classification of PQEs, specifically for the multiple nature PQEs. The intelligent techniques, such as artificial neural network (ANN) and support vector machine (SVM), become slow for detection of multiple nature PQEs due to the complex nature of features. The threshold values used for differentiating the different groups of PQEs and discriminating each PQE from a particular group of PQEs are selected by testing the algorithm on a large data set. A total of 110 disturbances for each PQE is simulated by changing the parameters, such as signal frequency, signal magnitude, disturbance magnitude, disturbance frequency, time incidence of a PQE, etc. Only those values are selected as threshold for which the PQEs are effectively classified during all the PQE data scenarios. A data set of 10 disturbances of PQE3 computed by variations of swell magnitude, signal frequency and time interval is included in Table 3. In a similar manner, a complete data set is computed using the simulation studies.

The classification is started using the CFI7 by grouping all the PQEs and CPQEs in two groups. PQEs with $CFI7 > 40$ are included in the PQE Group-1 (PG1), and PQEs with $CFI7 < 40$ are included in the PQE Group-2 (PG2).

PQEs and CPQEs included in PG1 are further classified using CFI1 in two groups: PG11 and PG12. PQEs and CPQEs with $CFI1 > 35$ are included in the category of PG11 and events with $CFI1 < 35$ are included in the category of PG12. CPQEs included in the group PG11 are further classified one by one using various decision rules which are illustrated in Figure 21. PQEs and CPQEs included in the group PG12 are further classified one by one using various decision rules which are illustrated in Figure 21.

PQEs and CPQEs included in PG2 are further classified using CFI7 in two groups: PG21 and PG22. PQEs and CPQEs with $CFI7 > 700$ are included in the category of PG21 and events with $CFI7 < 700$ are included in the category of PG22. CPQEs included in the group PG21 are further classified one by one using various decision rules illustrated in Figure 21. PQEs and CPQEs included in the group PG22 are further classified one by one using various decision rules illustrated in Figure 21.

Table 3. Magnitude of CFIs for voltage swell (PQE3).

S. No.	Type of Data Set	PQE Classification Index						
		CFI1	CFI2	CFI3	CFI4	CFI5	CFI6	CFI7
1	10% Swell with 50 Hz Frequency & 0.08 s time interval	44.1925	256.4699	0.0103	0.0341	3.9177	1.3301	14.1702
2	20% Swell with 50 Hz Frequency & 0.08 s time interval	46.0846	263.0518	0.0104	0.0352	4.0124	1.3505	15.2005
3	25% Swell with 50 Hz Frequency & 0.08 s time interval	48.0005	266.0879	0.0105	0.0367	4.0324	1.3710	15.1632
4	30% Swell with 50 Hz Frequency & 0.08 s time interval	48.879	267.2578	0.0105	0.0369	4.0892	1.3805	15.859
5	10% Swell with 60 Hz Frequency & 0.08 s time interval	43.872	255.0618	0.0103	0.0339	3.8902	1.3298	14.1005
6	20% Swell with 60 Hz Frequency & 0.08 s time interval	46.0001	263.0005	0.0103	0.0350	3.9998	1.3486	15.1720
7	25% Swell with 60 Hz Frequency & 0.08 s time interval	48.825	265.0825	0.0105	0.0365	4.0102	1.3682	15.0285
8	30% Swell with 60 Hz Frequency & 0.08 s time interval	48.0589	266.4086	0.0105	0.0368	4.0725	1.3799	15.7281
9	10% Swell with 50 Hz Frequency & 0.04 s time interval	44.1021	256.4102	0.0103	0.0340	3.9176	1.3300	14.1700
10	20% Swell with 50 Hz Frequency & 0.10 s time interval	46.0002	263.0101	0.0104	0.0350	4.0138	1.3504	15.1089

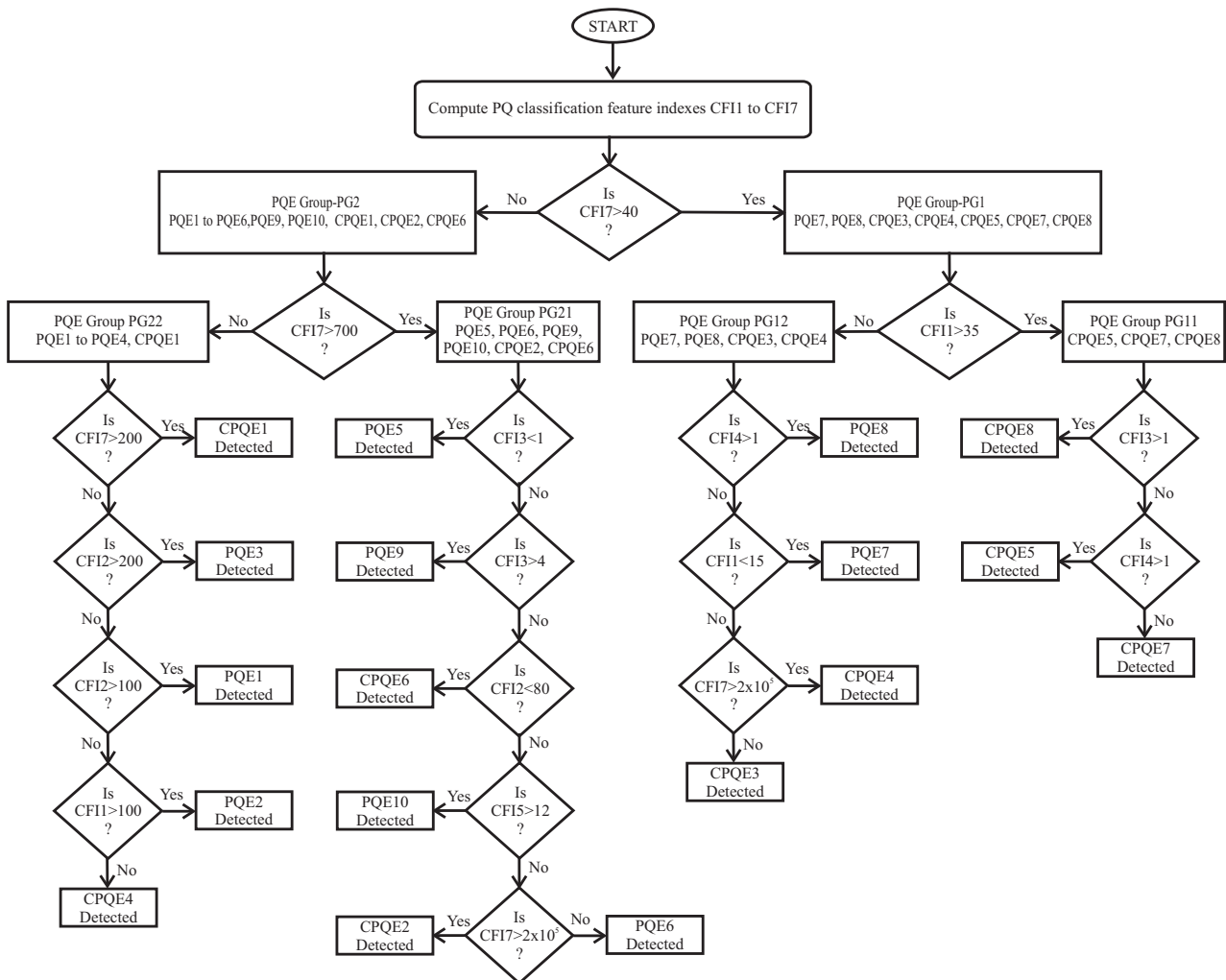


Figure 21. Classification tree for PQEs.

Accuracy of the method is computed by evaluating the number of accurately and inaccurately categorized PQEs and CPQEs. A total of 110 disturbances of each PQE are simulated by changing the various parameters, such as frequency, magnitude, time of

incidence, etc. Accurately categorized, inaccurately categorized and percentage accuracy to categorize the PQEs in a noise free environment and an environment of 20 dB SNR noise level is elaborated in Table 4. The average accuracy of the method is computed by averaging the accuracy of the categorization for all the PQEs and CPQEs. The first summation of categorization accuracy of all PQEs and CPQEs is computed and the result is divided by 18 to compute the average categorization accuracy of the proposed method. It is inferred from Table 4 that the proposed method is effective to categorize the PQEs with an accuracy of 98.58% in the noise-free scenario and 97.62% accuracy in the noisy scenario of 20 dB SNR.

Table 4. Accuracy of the proposed method for categorization of PQEs.

S. No.	Symbol of PQE	Nos. of Tested PQEs		Nos. of Accurate PQEs		Nos. of Inaccurate PQEs		Categorization Accuracy (%)	
		without Noise	Noise Present	without Noise	Noise Present	without Noise	Noise Present	without Noise	Noise Present
1	PQE1	110	110	110	110	0	0	100	100
2	PQE2	110	110	110	110	0	0	100	100
3	PQE3	110	110	110	110	0	0	100	100
4	PQE4	110	110	110	110	0	0	100	100
5	PQE5	110	110	107	105	3	5	97.27	95.45
6	PQE6	110	110	106	104	4	6	96.36	94.54
7	PQE7	110	110	110	110	0	0	100	100
8	PQE8	110	110	110	110	0	0	100	100
9	PQE9	110	110	109	108	1	2	99.09	98.18
10	PQE10	110	110	108	107	2	3	98.18	97.27
11	CPQE1	110	110	110	109	0	1	100	99.09
12	CPQE2	110	110	106	102	4	8	96.36	92.73
13	CPQE3	110	110	108	108	2	2	98.18	98.18
14	CPQE4	110	110	108	107	2	3	98.18	97.27
15	CPQE5	110	110	109	108	1	2	99.09	98.18
16	CPQE6	110	110	108	108	2	2	98.18	98.18
17	CPQE7	110	110	107	104	3	6	97.27	94.54
18	CPQE8	110	110	106	103	4	7	96.36	93.63
Average percentage Accuracy (%)								98.58	97.62

6. Validation of PQE Recognition on Real-Time Data of a Distribution Utility Network

The proposed method is tested to detect a PQE of voltage sag created due to a line-to-ground (LG) fault event occurring on a 11 kV feeder emanating from a 33/11 kV grid sub-station (GSS) of the distribution network of Jaipur Vidyut Votaran Nigam Limited (JVVNL), India. The practical test distribution line (TDL) used for the study is illustrated in Figure 22. The distribution substation transformer (DST) represents the 33/11 kV distribution sub-station (DSS) where the distribution bus (DB)-1 is maintained at 33 kV voltage, and DB-2 is maintained at 11 kV voltage. The DST is rated at 8 MVA, 33/11 kV. This DSS is connected to three 33 kV lines which emanate from the 132/33 kV grid sub-stations (GSS) of the utility grid. Hence, the utility grid represents the large area network of the power system. DB-3 is maintained on 11 kV. An aluminium conductor steel reinforced (ACSR) conductor is used for the practical 11 kV distribution line connecting DB-2 and DB-3. Details of the ACSR conductor are included in Table 5. The distribution transformer (DT) is rated at 60 kVAR and 11/0.44 kV. DB-4 is operated at 0.44 kV, and the load which is being fed from the DT is represented by distribution load (DL) connected on DB-4. DL is recorded equal to 28.14 kVAR at the time of taking the practical data of the LG fault. The primary distribution load (PDL) which is being fed from the DSS on 11 kV is represented by PDL which is equal to 3.78 MVA at the time of data recording.

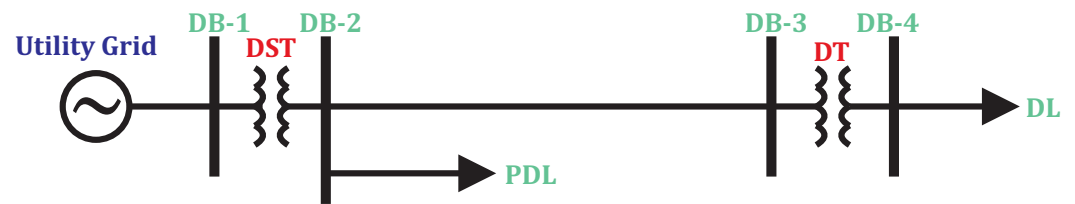


Figure 22. Test practical distribution line.

Table 5. Technical specifications of ACSR conductor of 11 kV overhead lines.

S. No.	Technical Parameter	Quantity
1	Overall conductor diameter	14.15 mm
2	Total conductor sectional area	118.5 mm ²
3	Total weight of conductor	394 kg/km
4	Breaking load of conductor	3270 daN
5	DC resistance of conductor at 20 °C	0.2733 Ω/km
6	Current Rating of conductor	270 A

Voltage data for a period of 12-cycle duration are collected from the disturbance recorder installed on bus DB-2 of the distribution system. These data are analyzed using the proposed method. The voltage waveform, the CPDI and the LPDI are illustrated in Figure 23a–c, respectively.

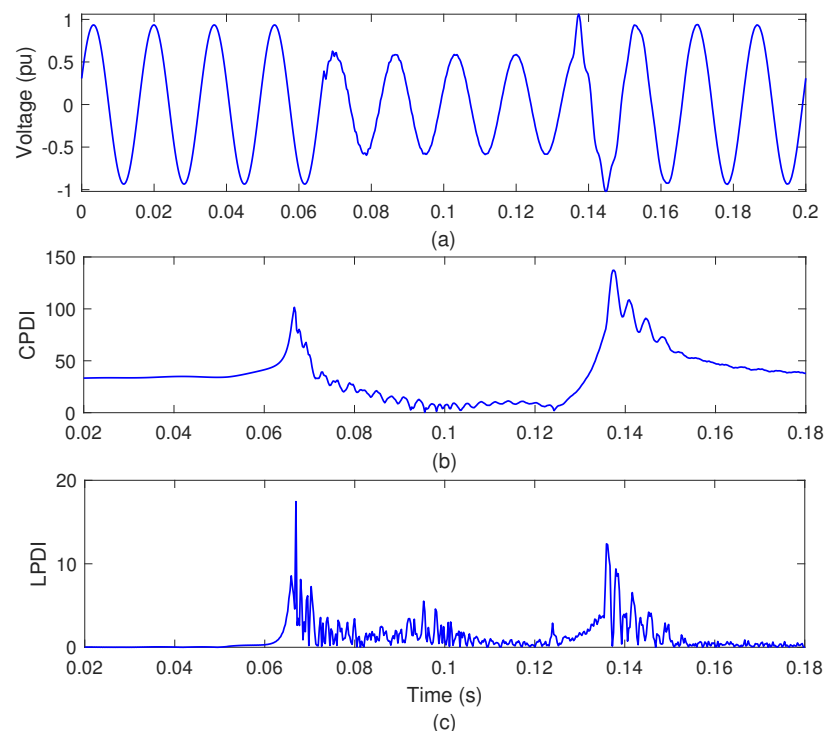


Figure 23. Detection of sag PQE due to a fault event: (a) voltage waveform; (b) CPDI; (c) LPDI.

Figure 23a details that a sag event is associated with the voltage waveform. Figure 23b details that the voltage sag is effectively detected by the decreased magnitude of the CPDI and high magnitude peaks at the time of the start and the end of a sag in voltage. Figure 23c details that high magnitude peaks at the time of the start and the end of the sag event localized the sag in the time domain.

7. Performance Comparative Study

The performance of the proposed PQ recognition technique is compared with a DWT-based technique available in [24]. The performance comparative study of the techniques considering different parameters is compiled in Table 6. It is established that the PQ spotting technique investigated in this paper performs better compared to the DWT-based method in terms of detection of changes in the frequency and voltage magnitude of the signal. The accuracy of the PQ classification of the investigated method is 98.58% in the noise-free environment which is higher compared to the DWT-based method which has 95.28% accuracy. Accuracy of the PQ classification of the investigated method is 97.62% in the noisy scenario which is higher compared to the DWT-based method which has 92.84% accuracy. The maximum computational time of PQ detection for the investigated method is 0.080564 s which is lower than the DW-based method which has a computational time of 0.3032 s. The investigated method is effective to detect PQ events of multiplicity four, whereas the DWT method is effective to recognize PQEs of multiplicity one.

Table 6. Comparative study of the proposed method with the DWT-based method.

S. No.	Comparison Parameter	Proposed Method	DWT Method [24]
1	Accuracy of classification without noise	98.58%	95.28%
2	Accuracy of classification with 20 dB SNR noise	97.62%	92.84%
3	Maximum computational time of PQ detection	0.080564 s	0.3032 s
4	Multiplicity of PQE which can be effectively detected	4	1

8. Conclusions

This paper investigated a PQ detection and categorization algorithm actuated by multiple signal processing techniques (ST, HT and DWT) and RBDT. A voltage waveform with a PQE is processed using the ST and the HT to compute the SPDI and the HPDI, respectively. A voltage waveform is decomposed using DWT to compute CFIs. A CPDI is computed from SPDI, HPDI and CFIs. The CPDI is used for the detection of PQEs. The LPDI is proposed to locate the PQEs in the time domain. The LPDI is computed by differentiating the CPDI with respect to time. An RBDT-based classifier driven by the CFIs is used for categorization of different PQEs. It is concluded that the CPDI effectively detects the PQEs, such as sag, swell, MI, harmonics, flicker, notches, spikes, IT, OT and combined PQEs, with multiplicity of two, three and four. Further, it is also concluded that the designed RBDT-based classifier using the CFIs as input features is effective to categorize the PQEs and CPQEs with an accuracy of 98.58% in a noise-free environment and 97.62% in the presence of 20 dB SNR noise with low computational time of 0.080564 s. Accuracy as high as intelligent techniques has been achieved using the simple nature RBDT classifier. The designed PQ recognition algorithm has the advantages that the weight factor has been replaced by the features computed from the PQE signal, and the computational burden is reduced. The algorithm is also effective to detect a sag PQ event due to an LG fault incident on a practical distribution utility network. A comparative study of the investigated method with a DWT-based technique is performed, and it is established that the investigated method performs better compared to the DWT in terms of accuracy of classification with and without noise, maximum computational time of PQ detection and multiplicity of PQE which can be effectively detected. The designed algorithm can effectively be deployed in online PQ monitoring devices.

Author Contributions: Conceptualization, S.S.; methodology, S.S.; software, S.S. and O.P.M.; validation, S.S. and O.P.M.; formal analysis, S.S. and O.P.M.; investigation, S.S.; resources, I.B., B.N., A.A. and B.K.; data curation, S.S. and O.P.M.; writing—original draft preparation, S.S.; writing—review and editing, S.S., O.P.M., B.K. and A.A.; visualization, I.B., B.N., B.K. and J.B.B.; supervision, A.S., A.R.G. and J.B.B. All authors have read and agreed to the published version of the manuscript.

Funding: This research received no external funding.

Institutional Review Board Statement: Not applicable.

Informed Consent Statement: Not applicable.

Data Availability Statement: Research data will be provided by corresponding author on request.

Conflicts of Interest: There is no conflict of interest.

Abbreviations

Abbreviations used in this article are detailed below:

ACSR	Aluminium conductor steel reinforced
ANN	Artificial neural network
CFI	Classification feature index
CPDI	Combined PQ disturbance index
CPQE	Combined PQ event
DB	Distribution bus
DSS	Distribution sub-station
DL	Distribution load
DT	Distribution transformer
DTCWT	Dual Tree Complex Wavelet Transform
DWT	Discrete Wavelet transform
EWT	Empirical wavelet transform
FFT	Fast Fourier transform
GSS	Grid sub-station
HPDI	Hilbert PQ disturbance index
HT	Hilbert transform
IT	Impulsive transient
JVVNL	Jaipur Vidyut Vitaran Nigam Limited
LG	Line to ground fault
LPDI	Location PQ disturbance index
MI	Momentary interruption
MST	Modified Stockwell transform
OT	Oscillatory transient
PDL	Primary distribution load
PQ	Power quality
PQE	Power quality event
RBDT	Rule based decision tree
RES	Renewable energy sources
SNR	Signal to noise ratio
SOM	Stockwell output matrix
SOMA	Matrix of absolute values of SOM
SPDI	Stockwell PQ disturbance index
SSI	Stockwell summation index
SSPQD	Single shot PQ detection
ST	Stockwell transform
SVM	Support vector machine
TDL	Practical test distribution line

References

1. Subudhi, U.; Dash, S. Detection and classification of power quality disturbances using GWO ELM. *J. Ind. Inf. Integr.* **2021**, *22*, 100204. [[CrossRef](#)]
2. Khetarpal, P.; Tripathi, M.M. A critical and comprehensive review on power quality disturbance detection and classification. *Sustain. Comput. Inform. Syst.* **2020**, *28*, 100417. [[CrossRef](#)]
3. Mahela, O.P.; Shaik, A.G.; Gupta, N. A critical review of detection and classification of power quality events. *Renew. Sustain. Energy Rev.* **2015**, *41*, 495–505. [[CrossRef](#)]
4. Bonde, G.; Paraskar, S.; Jadhao, S. Review on detection and classification of underlying causes of power quality disturbances using signal processing and soft computing technique. *Mater. Today Proc.* **2022**, *58*, 509–515. [[CrossRef](#)]

5. Kapoor, R.; Saini, M.K. Hybrid demodulation concept and harmonic analysis for single/multiple power quality events detection and classification. *Int. J. Electr. Power Energy Syst.* **2011**, *33*, 1608–1622. [[CrossRef](#)]
6. Deokar, S.; Waghmare, L. Integrated DWT–FFT approach for detection and classification of power quality disturbances. *Int. J. Electr. Power Energy Syst.* **2014**, *61*, 594–605. [[CrossRef](#)]
7. Iturrino-García, C.; Patrizi, G.; Bartolini, A.; Ciani, L.; Paolucci, L.; Luchetta, A.; Grasso, F. An Innovative Single Shot Power Quality Disturbance Detector Algorithm. *IEEE Trans. Instrum. Meas.* **2022**, *71*, 1–10. [[CrossRef](#)]
8. Shaik, R.S.; Kumar, R.; Asif, M.; Yadav, D. DTCWT-SVM Based Identification of Single and Multiple Power Quality Disturbances. In Proceedings of the 2022 International Conference on Intelligent Controller and Computing for Smart Power (ICICCSPP), Hyderabad, India, 21–23 July 2022; pp. 1–6. [[CrossRef](#)]
9. Sakib, M.S.; Islam, M.R.; Tanim, S.M.S.H.; Alam, M.S.; Shafiullah, M.; Ali, A. Signal Processing-based Artificial Intelligence Approach for Power Quality Disturbance Identification. In Proceedings of the 2022 International Conference on Advancement in Electrical and Electronic Engineering (ICAEEE), Gazipur, Bangladesh, 24–26 February 2022; pp. 1–6. [[CrossRef](#)]
10. Carní, D.L.; Lamonaca, F. Toward an Automatic Power Quality Measurement System: An Effective Classifier of Power Signal Alterations. *IEEE Trans. Instrum. Meas.* **2022**, *71*, 1–8. [[CrossRef](#)]
11. Jamlu, N.U.I.A.; Shahbudin, S.; Kassim, M. Power Quality Disturbances Classification Analysis Using Residual Neural Network. In Proceedings of the 2022 IEEE 18th International Colloquium on Signal Processing & Applications (CSPA), Selangor, Malaysia, 12 May 2022; pp. 442–447. [[CrossRef](#)]
12. Swarnkar, N.K.; Mahela, O.P.; Lalwani, M. Estimation of Power Quality in Distribution System with High Penetration of Renewable Power Generation. In Proceedings of the 2021 Innovations in Power and Advanced Computing Technologies (i-PACT), Kuala Lumpur, Malaysia, 27–29 November 2021; pp. 1–6. [[CrossRef](#)]
13. Su, D.; Li, K.; Shi, N. Power Quality Disturbances Recognition Using Modified S-Transform Based on Optimally Concentrated Window with Integration of Renewable Energy. *Sustainability* **2021**, *13*, 9868. [[CrossRef](#)]
14. Mozaffari, M.; Doshi, K.; Yilmaz, Y. Real-Time Detection and Classification of Power Quality Disturbances. *Sensors* **2022**, *22*, 7958. [[CrossRef](#)] [[PubMed](#)]
15. Chen, S.; Li, Z.; Pan, G.; Xu, F. Power Quality Disturbance Recognition Using Empirical Wavelet Transform and Feature Selection. *Electronics* **2022**, *11*, 174. [[CrossRef](#)]
16. Tan, R.H.; Ramchandaramurthy, V.K. Numerical model framework of power quality events. *Eur. J. Sci. Res.* **2010**, *43*, 30–47.
17. Mahela, O.P.; Shaik, A.G. Recognition of power quality disturbances using S-transform based ruled decision tree and fuzzy C-means clustering classifiers. *Appl. Soft Comput.* **2017**, *59*, 243–257. [[CrossRef](#)]
18. Čurović, L.; Murovec, J.; Novaković, T.; Prislán, R.; Prezelj, J. Stockwell transform for estimating decay time at low frequencies. *J. Sound Vib.* **2021**, *493*, 115849. [[CrossRef](#)]
19. Arranz, R.; Ángel Paredes.; Rodríguez, A.; Muñoz, F. Fault location in Transmission System based on Transient Recovery Voltage using Stockwell transform and Artificial Neural Networks. *Electr. Power Syst. Res.* **2021**, *201*, 107569. [[CrossRef](#)]
20. Carneiro, E.; Das, M.K.; Florea, A.; Kumchev, A.V.; Malik, A.; Milinovich, M.B.; Turnage-Butterbaugh, C.; Wang, J. Hilbert transforms and the equidistribution of zeros of polynomials. *J. Funct. Anal.* **2021**, *281*, 109199. [[CrossRef](#)]
21. Wang, W.; Liang, J.; Liu, R.; Song, Y.; Zhang, M. A Robust Variable Selection Method for Sparse Online Regression via the Elastic Net Penalty. *Mathematics* **2022**, *10*, 2985. [[CrossRef](#)]
22. Mohamed, M.S.; Barakat, H.M.; Alyami, S.A.; Abd Elgawad, M.A. Cumulative Residual Tsallis Entropy-Based Test of Uniformity and Some New Findings. *Mathematics* **2022**, *10*, 771. [[CrossRef](#)]
23. Rice, J.A. *Mathematical Statistics and Data Analysis*; Cengage Learning: London, UK, 2006.
24. Dekhandji, F.Z. Detection of power quality disturbances using discrete wavelet transform. In Proceedings of the 2017 5th International Conference on Electrical Engineering-Boumerdes (ICEE-B), Boumerdes, Algeria, 29–31 October 2017; pp. 1–5. [[CrossRef](#)]

Disclaimer/Publisher’s Note: The statements, opinions and data contained in all publications are solely those of the individual author(s) and contributor(s) and not of MDPI and/or the editor(s). MDPI and/or the editor(s) disclaim responsibility for any injury to people or property resulting from any ideas, methods, instructions or products referred to in the content.